Schlecht Stephen (Orcid ID: 0000-0002-6857-927X)
Surowiec Rachel (Orcid ID: 0000-0001-7614-4412)
Kozloff Kenneth (Orcid ID: 0000-0002-1108-7258)

Gene Expression Profile and Acute Gene Expression Response to Sclerostin Inhibition in Osteogenesis Imperfecta Bone

Rachel K. Surowiec, PhD [1,2], Lauren F. Battle, BSc [2], Stephen H. Schlecht, PhD [2,3], Edward M. Wojtys, MD [2], Michelle S. Caird, MD [2], Kenneth M. Kozloff, PhD[1,2]

[1] Department of Biomedical Engineering, University of Michigan, Ann Arbor, Michigan, USA

[2] Department of Orthopaedic Surgery, University of Michigan, Ann Arbor, Michigan, USA

[3] Department of Mechanical Engineering, University of Michigan, Ann Arbor, Michigan, USA

Corresponding Author:

Kenneth M. Kozloff, PhD

University of Michigan Orthopaedic Research Laboratories

2015 Biomedical Science Research Building

109 Zina Pitcher Place

Ann Arbor, Michigan 48109-2200

Phone: +1(734) 936-2158

Fax: (734) 647-0003

Email: Kenkoz@umich.edu

This is the author manuscript accepted for publication and has undergone full peer review but has not been through the copyediting, typesetting, pagination and proofreading process, which may lead to differences between this version and the Version of Record. Please cite this article as doi: 10.1002/jbm4.10377

Abstract

Sclerostin antibody (SclAb) therapy has been suggested as a novel therapeutic approach toward addressing the fragility phenotypic of osteogenesis imperfecta (OI). Observations of cellular and transcriptional responses to SclAb in OI have been limited to mouse models of the disorder, leaving a paucity of data into the human OI osteoblastic cellular response to the treatment. Here, we explore factors associated with response to SclAb therapy *in vitro* and in a novel xenograft model using OI bone tissue derived from pediatric patients.

Bone isolates (~2 mm^3) from OI patients (OI Type III, Type III/IV and Type IV, n=7; non-OI control, n=5) were collected to media, randomly assigned to an untreated (UN), low-dose SclAb (TRL, 2.5 μg/mL), or high-dose SclAb (TRH, 25 μg/mL) group and maintained *in vitro* (37°C). Treatment occurred on day 2 and 4 and removed on day 5 for TaqMan qPCR analysis of genes related to the *Wnt* pathway. A subset of bone was implanted subcutaneously into an athymic mouse, representing our xenograft model, and treated (25 mg/kg s.c. 2x/wk for 2/4wks). Implanted OI bone was evaluated using μCT and histomorphometry.

Expression of *Wnt/Wnt*-related targets varied among untreated OI bone isolates. When treated with SclAb, OI bone demonstrated an upregulation in osteoblast and osteoblast progenitor markers which was heterogeneous across tissue. Interestingly, the greatest magnitude of response generally corresponded to samples with low untreated expression of progenitor markers. Conversely, samples with high untreated expression of these markers demonstrated a lower response to treatment. *In vivo* implanted OI bone demonstrated a bone forming response to SclAb via μCT and corroborated by histomorphometry. SclAb induced downstream *Wnt* targets *WISP1* and *TWIST1* and elicited a

compensatory response in *Wnt* inhibitors *SOST* and *DKK1* in OI bone with the greatest magnitude from OI cortical bone.

Understanding patients' genetic, cellular, and morphological bone phenotypes may play an important role in predicting treatment response, thus aiding clinical decision making for pharmacological intervention to address fragility in OI.

Keywords: Osteogenesis Imperfecta, Sclerostin Antibody, Bone Formation, *Wnt* signaling, Anabolic therapy

Introduction

Osteogenesis imperfecta (OI) is a rare and severe congenital bone dysplasia characterized by low bone mass and poor bone quality with increased pathological fracture risk.[1] OI is both genetically and clinically heterogeneous; the bone dysplasia can currently be categorized into 18+ genetically unique types ranging in severity from mild forms with minor skeletal clinical manifestations to perinatally lethality.[2-4] Further complicating the disease are the different possible modes of inheritance (dominant, recessive or X-linked gene mutations) and variability associated with the affected genetic loci resulting in the range of phenotypic presentation. [5] Further, patients with the same OI-causing mutation can present with different clinical phenotypes. [6] In up to 85% of cases, OI is caused from a mutation in the *COL1A1* or *COL1A2* encoding the α1 or α2 chain of type I collagen respectively, resulting in an underproduction of normal collagen or secretion of defective collagen chains depending on the mutation.[7-9] More recently, other proteins localized in the matrix, endoplasmic reticulum (ER), ER-golgi, and nucleus have been identified in the pathogenesis of OI and make up the remaining 15% of cases.[3, 9-20] This spectrum of genotype-phenotype variability has made both diagnosis and management of the disease challenging; as such, no cure for OI exists, there is no United States Food and Drug Administration or European Medicines Agency approved pharmacological treatment and consensus on an appropriate treatment strategy has yet to be identified. [21, 22]

Pharmacologic treatment strategies for OI have evolved from approaches developed to treat osteoporosis, a metabolic bone disease. These strategies aimed at eliciting an increase in bone mass, an improvement in architecture and a decrease in fracture risk, often result in a variable clinical response when applied to OI. Current clinical pharmacological approaches to manage OI relies on anti-resorptive

bisphosphonates, yet bisphosphonates have demonstrated variable patient outcomes depending on OI phenotype, severity and bone site.[23, 24] Further, long-term bisphosphonate use in pediatric OI is a concern due to its suppression of bone turnover and the drug's long half-life which leads to long-term residence in the bone. [25] Inconsistent clinical pediatric OI results have also been reported with Denosumab, a RANKL inhibitor, and concerns regarding hypercalciuria development during active therapy observed in pre-clinical studies have limited its clinical use. [26-28] More recently, bone-forming sclerostin antibody (SclAb) has emerged as a promising alternative or adjuvant to existing therapies and acts by inhibiting sclerostin, a negative regulator of bone formation. {Li, 2014 #58} SclAb has elicited significant increases in bone mineral density (BMD) and quality during clinical trials for post-menopausal osteoporosis [29, 30] and stimulated markers of bone formation, reduced resorption and increased lumbar spinal areal BMD in adults with moderate OI (limited to type I, III, or IV). [31]

Despite these findings, effects in the pediatric OI population and across all OI types remain unknown. Different OI phenotypes appear to respond differently to therapies. Pre-clinically, the bone-forming response to SclAb has varied in magnitude from strong in the moderate knock-in Brtl/+ murine model, moderate in the recessive severe Crtap$^{-/-}$ murine model, and a lower bone-forming response in the dominant severe Col1a1 $^{jrt/+}$ murine model.[32-36] Therefore, factors that contribute to the heterogeneity of the disorder, including skeletal morphology and untreated gene expression profile may play an important role in the patient's response to therapy.

Understanding the transcriptional response to treatment in the diseased target tissue is of great interest. Gene expression response following SclAb treatment has been reported in rat models of post-

menopausal osteoporosis and in female Balb/c mice, [37-40] highlighting the unique signaling events and compensatory response occurring in the osteoblast lineage as a result of SclAb. However, patterns of gene expression response due to treatment in human OI bone tissue remains unknown and difficult to assess clinically. We sought to evaluate gene expression profiles in native pediatric OI bone tissue and describe the acute gene expression response to SclAb treatment across OI patients with severe and moderate phenotypes at a variety of anatomic sites and bone types. We explore how the samples' untreated cellular condition and baseline morphological phenotype contribute to treatment response during acute sclerostin inhibition.

Materials and Methods

Study Design

Seven pediatric OI patients undergoing corrective surgical orthopaedic intervention were prospectively enrolled and the subject and/or legal guardian provided informed consent for this Institutional Review Board approved study. Five additional age-matched pediatric non-OI deidentified patients undergoing anterior cruciate ligament (ACL) reconstruction as a result of sport-related injury were recruited and tissue was considered exempt by the Institutional Review Board. Detailed subject demographics including OI type and bone harvest location can be appreciated in **Table 1**. Native bone typically discarded as surgical waste was collected immediately to media (αMEM/10% fetal bovine serum (FBS)) and placed on ice for experimental preparation. Bone tissue was divided into a Falcon 12-

well microplate (Corning Inc., Corning, New York) with each well containing 3 mL of media and maintained in culture at 37°C. Each well contained one solid bone isolate ~2 mm^3 in size and each donor yielded up to 14 usable bone isolates (**Table 1).** Bone was randomly assigned to an untreated (UN), treated with a low dose of SclAb (TRL, 2.5 μg/mL), or treated with a high dose of SclAb (TRH, 25 μg/mL) condition. Each donor had enough bone tissue to repeat each UN, TRL, TRH condition 2-4 times. Wells containing tissue and media were dosed directly with SclAb on days two and four and all samples were removed on day five to 1 mL of TRIzol reagent (Invitrogen, Carlsbad, CA) and kept at -80°C until RNA isolation occurred. For all conditions, media was changed on day two and four prior to treatment. One bone sample from each donor was fixed immediately in 10% neutral buffered formalin (NBF) for 24 hours, decalcified in 10% ethylenediaminetetracetic acid (EDTA) for 15-20 days, paraffin processed and stained with hematoxylin and eosin (H&E) to determine bone morphology using established procedures.[41]. A detailed schematic can be found in **Figure 1A**.

Due to the amount of donor bone tissue procured, a subset of bone tissue from patients OI3, OI4 and OI6 were collected to media and immediately implanted subcutaneously on the dorsal surface of an athymic mouse ($Foxn^{nu}$ [002019]; The Jackson Laboratory, Bar Harbor, ME, USA) representing our xenograft model to evaluate the effects of SclAb in a host-derived system more closely recapitulating the *in vivo* microenvironment (**Figure 1B**) using the methods described in detail in Surowiec *et al.* [42] In short, fourteen bone samples in total were implanted and mice were randomly assigned to an untreated or SclAb treated group. SclAb treatment (25 mg/kg) was administered to the host (mouse) subcutaneously two times a week for either 2 or 4 weeks where the mice were euthanized by CO_2 inhalation followed by bilateral pnuemorthorax. All mice received calcein (30 mg/kg, intraperitoneal

(i.p.) injection), administered seven days before sacrifice and alizarin (30 mg/kg, i.p.) administered one day prior to sacrifice, to follow new bone formation. Implanted mice underwent μCT imaging (Bruker Skyscan 1176, Bruker BioSpin, Belgium) 24 hours following implantation and immediately following euthanasia using an X-ray voltage of 50 kV, 800 μA current and a 0.5 mm aluminum filter. Scans were reconstructed at an 18 μm isotropic voxel size and calibrated with the use of two manufacturer provided hydroxyapatite standards. The bone implant was manually segmented followed by a series of automated processes so that only implant was extracted and analyzed for longitudinal changes (presented as a percent change from pre- to post- scans) in bone surface (CTAn Version 1.15.4.0, Bruker Biospin, Belgium). Following imaging, OI bone tissue implants were removed from the host and plastic processed for histomorphometric analysis using standard laboratory procedure. All experimental animal procedures were approved by the University of Michigan Committee for the Use and Care of Animals.

Bone tissue preparation and RNA extraction

Total RNA was extracted from each bone isolate by first pulverizing each bone in 1 mL TRIzol using a high-speed tissue homogenizer (Model 1000; ThermoFisher Scientific). Each bone isolate underwent three 20-second cycles of homogenization and was placed on ice between cycles. The bone's total nucleic acid content was isolated using 0.2 mL of 24:1 chloroform:isoamyl alcohol per 1 mL of TRIzol, centrifuged at 12000 g for 15 minutes at 4°C where the supernatant containing the RNA fraction was removed by pipetting. RNA was then purified using the RNeasy Mini Kit (Qiagen, Valencia, California) followed by DNA digestion with an RNase-Free DNase Set (Qiagen) following instructions

supplied by the manufacturer. Finally, total RNA was eluted in 30 µL of RNase-free water. For quality control, RNA concentration extracted from each bone isolate was determined using NanoDrop 2000 (ThermoFisher Scientific) followed by assessment of RNA quality using a bioanalyzer (Model 2100, Pico Kit; Agilent Technologies, Santa Clara, California) to generate an RNA integrity number (RIN). In order to maximize nucleic acid content from each patient condition, RNA from each well condition (UN, TRL, TRH) per patient with an RNA integrity number (RIN) of 5.5 or greater were pooled to yield 200 ng per condition and a new concentration value was determined using the NanoDrop. The RIN number of 5.5 was chosen due to the rarity of the human tissue and few samples did not meet this threshold; two non-OI and four OI bone samples had RIN values below 5.5 and were excluded from analysis and not pooled as they did not meet our quality standard for the study. The average RIN number was 8.8; pooled non-OI bone RIN values ranged from 6.3-10 and OI patient bone from 6.7-9.9. Extracted RNA was stored at -80°C until further processing.

TaqMan qPCR analysis

The expression levels of 10 genes related to the canonical and non-canonical *Wnt* signaling pathway and one endogenous control were quantified using TaqMan quantitative real-time polymerase chain reaction (RT-qPCR) (**Table 2)**. Specifically, downstream *Wnt* targets (*WISP1*, *TWIST1*), inhibitory regulators of bone formation (*SOST*, *DKK1*), markers of osteoblastogenesis (*SP7*, *RUNX2*), osteoblast markers (*BGLAP*, *COL1A1*), and markers of osteoclast differentiation and activity (*OPG*, *RANKL*) were evaluated. The panel represents a subset of markers in the bone remodeling cycle many of which have been identified as key targets for SclAb therapy in prior animal studies.[37-39, 43] Due to

the rarity of the OI bone tissue and the size of the available harvested bone (which affected the amount of total nucleic acid we were able to extract), we chose to analyze only one housekeeping gene (*HPRT1*), which has been documented in the literature as a stable gene across experimental conditions in human bone studies. [44, 45]

Pooled, purified RNA samples underwent reverse transcription using qScript cDNA SuperMix (Quanta Biosciences, Gaithersburg, MD) using 1.5 μg of retro-transcribed RNA per reaction followed by thermocycling (C1000 Thermal Cycler, Bio-Rad Laboratories, Hercules, California) according to manufacturer recommendations. TaqMan Gene Expression Master Mix (Applied Biosystems) was combined with cDNA and validated TaqMan primer (Applied Biosystems, Foster City, California) and loaded into a 96-well microfluidic array card (Applied Biosystems, Foster City, California). Each array card permitted for two patients' (one OI, one non-OI) samples (UN, TRL, TRH, each) and five primers plus the housekeeping primer simultaneously with twelve array cards in total evaluated. All reactions were run in duplicate and a no-template control and no-reverse transcription control were utilized. Array cards were centrifuged at 4°C (Legend XTR (with custom TaqMan array card bucket); Sorvall, Waltham, Massachusetts), sealed and ran in accordance to recommendations from the manufacturer.

Amplification plots were generated and expression of *SOST, DKK1, COL1A1, BGLAP, OPG, RANKL, RUNX2, TWIST1, WISP1,* and the housekeeping gene *(HPRT1)* were quantified. Baseline and threshold settings were adjusted to obtain an accurate threshold cycle (CT) that was standard across all patients (OI 1-7 and non-OI 1-5) and conditions (UN, TRL, TRH) per each individual gene of interest in order to understand baseline cellular expression levels of the donor tissue and treatment response to

SclAb. Comparative CT method (ΔΔCT) was used to calculate fold change expression levels by normalizing data to endogenous *HPRT1* by averaging the duplicates of the gene of interest and the duplicate of the housekeeping gene for each patient per condition.[46] Experiments in which duplicate reactions deviated by four or more cycles (CT) were deemed a failed reaction due to technical error and thus excluded.

The individual OI patient UN condition was normalized to the average non-OI UN condition (control) to quantify variability in untreated OI gene expression and to provide a snapshot of genotypic variability present among the cohort of harvested OI patient samples irrespective of OI clinical phenotype. We then quantified the individual patient response to SclAb by normalizing each individual patient sample's treatment condition (TRL, TRH) to that patient sample's untreated condition to assess treatment response variation among individual patient tissue. Next, we evaluated the response to SclAb by clinical phenotype by averaging the treatment condition (TRL, TRH) normalized to the average untreated condition within each OI type (Type III, Type III/IV, Type IV). Finally we normalized each mean treatment condition (TRL, TRH) within OI type to the mean untreated non-OI control allowing observations on whether SclAb treatment returned gene expression to non-OI untreated control levels.

Statistical Analysis

All data were analyzed using GraphPad Prism v7 (GraphPad Software, La Jolla, California). Gene expression results are shown as mean ± standard error of the mean (SEM). Differences in individual OI untreated gene expression, individual OI treatment response and mean treatment response within OI type were statistically evaluated via a paired t-test using the respective ΔCT values as

described in detail by Yuan et al. [47] A two-way ANOVA (non-repeated measures) with patient type (OI Type III, OI Type III/IV, OI Type IV or Non-OI) and treatment (UN, TRL, TRH) as factors was used to determine differences in treatment response to SclAb by patient group. Follow-up Dunnett's post-hoc analysis was used where appropriate in order to compare average OI patient condition outcomes back to the average non-OI untreated controls. TaqMan probes have validated amplification specificity, sensitivity and efficiency; as such fold changes from the TaqMan assays (up or down) of 1.5 or greater that were identified as being statistically significant ($p < 0.05$) via paired t-test or two-way ANOVA met our criteria for denoting differences in gene expression levels. [48]

Results

Bone samples harvested from OI patients were of cortical and trabecular origin, while harvested non-OI bone originating from metaphyseal tibial tunnel samples during anterior cruciate ligament (ACL) reconstruction were morselized trabecular bone pieces approximately 1-2 mm^3 (**Figure 2**). Donor-derived bone yield varied, ranging from 5-14 usable samples; subjects with lower sample yield ultimately resulted in lower nucleic acid concentration which did not allow the evaluation of all conditions and/or all genes of interest. For these samples, an abbreviated panel of genes were evaluated or the TRL condition was omitted. When a gene or condition was omitted, missing fold-change values were denoted herein by "insufficient nucleic acid content" in the figures where appropriate.

Untreated Gene Expression was Heterogeneous among OI Patients

Untreated expression levels for all ten genes in each individual OI donor normalized to the average untreated non-OI control condition was conducted to understand genotypic variability among OI subjects. Untreated expression varied among the OI donors regardless of bone morphological or Sillence type **Figure 3**. OI bone generally demonstrated lower expression of downstream *Wnt* targets (*WISP1, TWIST1*). Inhibitory regulators (*SOST* and *DKK1*) were variable between OI. *SOST* expression for OI1 was significantly greater compared to non-OI controls (+5.54 fold difference). Osteoblast marker genes (*SP7, RUNX2*) and osteoblast progenitor marker genes (*BLGAP, COL1A1*) were heterogeneous among OI donors and were generally expressed below non-OI levels with some exceptions. OI5 (Type III/IV OI) demonstrated both high levels of inhibitory regulator *DKK1* and osteoclast precursor *RANKL* and high expression levels of osteoblast and progenitor (*SP7, BGLAP*) markers well above both non-OI controls and OI patients.

Individual OI donor response to SclAb varied in magnitude

Individual donor response to SclAb was evaluated using a low and high dose to understand response variability among donors. Differences in treatment response among OI donors can be appreciated in **Figure 4** where significance within each donor between conditions (UN, TRL, TRH) is denoted by stars and brackets. A bone-forming response to treatment observed by an upregulation of osteoblast activity was observed in nearly all OI samples regardless of bone type (trabecular, cortical) or OI Type (III, III/IV, IV). For *SP7*, treatment response was improved (through a greater upregulation) using the TRH dose compared to the TRL. For *RUNX2, BGLAP* and *COL1A1*, a dose dependent effect was less pronounced among OI donors in these osteoblast-related genes. SclAb induced an upregulation

in downstream *Wnt* targets (W*ISP1, TWIST1*) and an upregulation (compensatory response) in inhibitory regulators (*SOST, DKK1*). The greatest magnitude of upregulation was observed in treated OI cortical-derived bone tissue (OI2, OI3, OI6) for these targets.

Response to treatment appeared related to untreated gene expression levels

Untreated gene expression from each sample appears to influence the magnitude of response to SclAb treatment, specifically for osteoblast and osteoblast progenitor genes *COL1A1*, *RUNX2*, *SP7* and *BGLAP* (**Figure 5**). Data suggests that samples with the highest untreated osteoblast expression were least responsive to the acute SclAb treatment. This can be appreciated in the case of OI2 with high untreated expression of *SP7* (**Figure 3**) and down regulation (TRL) and nominal upregulation (TRH) with SclAb treatment (**Figure 4**). A similar observation was made in OI5 for *BGLAP* and OI1 for *RUNX2* and *COL1A1* genes (**Figure 3 and Figure 4**). In contrast, samples with low untreated osteoblast expression were the most responsive in bone formation markers to SclAb treatment (**Figure 5**). This can be appreciated in OI3, OI6 and OI7 which had the lowest untreated expression of *SP7* (**Figure 3**) and the greatest magnitude of upregulation with SclAb treatment (**Figure 4**). This observation was true regardless of dose for OI3 and OI6 and for low dose (TRL) for OI7. Similar observations were made for OI7 for genes *RUNX2*, *BGLAP*, *COL1A1* and for OI5 for *RUNX2* and *COL1A1* (**Figure 3 and Figure 5**). Further, individual samples with low untreated expression of downstream *Wnt* target *TWIST1* and inhibitory regulators *DKK1* and *SOST* relative to the untreated average non-OI controls demonstrated the largest magnitude of upregulation following SclAb treatment. The increased compensatory response of inhibitory regulators *DKK1* (OI3 and OI6) and *SOST* (OI6) with treatment in these samples correlated

with low untreated expression of these targets (untreated expression **Figure 3**, treatment response **Figure 4**). Conversely, high untreated expression for DKK1 in OI5 and SOST for OI1 demonstrated a moderate-to-low treatment response with SclAb (**Figure 3** and **Figure 4**) compared to other OI samples with more moderate-to-low untreated

Response to SclAb was also differential by patient's clinical Sillence type classification

To determine whether Sillence classification could predict SclAb response, mean SclAb treatment response was stratified by the patient's clinical Sillence classification by averaging the gene expression data from OI Type III, OI Type III/IV and OI Type IV patients, respectively (**Supplemental Figure 1**). Gene expression response to SclAb was heterogeneous among clinical OI phenotypes. OI Type III samples demonstrated a greater upregulation in *TWIST1*, *BGLAP* and *RUNX2* with treatment while OI Type III/IV had a greater magnitude of upregulation for *WISP1*, *SOST* and *COL1A1*. OI Type IV samples demonstrated the greatest upregulation in *DKK1*, *SP7* and a comparable response in *BGLAP* for OI Type III patients. There was no statistical significance reached in gene expression response within OI type.

Results from two-way ANOVA (non-repeated measures) and follow-up Dunnett's post-hoc testing for each gene of interest comparing average treatment condition (UN, TRL, TRH) within OI type (Type III, Type IV, or Non-OI) normalized to average non-OI untreated condition can be appreciated in **Supplemental Figure 2A-B**. Results revealed a significant effect of OI type for downstream *Wnt* target *TWIST1*, inhibitory regulators *SOST* and *DKK1* and osteoblastogenesis marker *RUNX2*. Additionally, a significant effect of treatment and a significant interaction between treatment and OI type was observed

for *SOST* (**Supplemental Figure 2A**). OI Type III samples were the only sample conditions which differed significantly from the non-OI untreated controls following SclAb treatment (**Supplemental Figure 2B**). Specifically, following treatment OI Type III samples had a significantly greater upregulation in *TWIST1* (TRL and TRH), *SOST*, (TRL and TRH), and *DKK1* (TRL) above non-OI untreated control levels. Following acute SclAb treatment, osteoblast and osteoblast precursor markers of *SP7*, *RUNX2*, *BGLAP* and *COL1A1* were upregulated to- or above non-OI untreated control levels in OI type III samples.

In vivo treatment confirmed a bone forming response to SclAb

The subset of OI bone samples from OI3, OI4 and OI6 implanted into our xenograft model demonstrated increases in μCT measures of percent change bone surface (BS) following SclAb treatment at 2 (OI3, OI4, OI6) and 4 weeks (OI4) (**Figure 6A**). Two week treated implants demonstrated the most robust increase in bone surface (+ 29%) followed by four weeks of treatment which increased on average by +12%. Untreated implants demonstrated a mean -3% decrease in BS following the implantation duration at two weeks and a slight increase (+10%) following untreated implantation at four weeks. Histomorphometry corroborated μCT findings. Implants following two and four weeks of treatment demonstrated robust calcein and alizarin fluorochrome labeling compared to the untreated implants which had minimal non-specific calcein labeling only (**Figure 6B**).

Discussion

In this study we explored the impact of SclAb on OI bone cells within their native extracellular environment using a panel of 10 key *Wnt*-related bone targets. Gene expression was heterogeneous across untreated conditions both between and within the patient's phenotypic clinical classification. Acute SclAb treatment induced upregulation of osteoblast activity in nearly all OI samples regardless of bone origin (trabecular, cortical) or OI Type (III, III/IV, or IV) and response varied in magnitude across subject samples. When the average condition response by OI type was normalized to the average non-OI untreated controls, SclAb upregulated osteoblast marker and progenitor genes in OI Type III subjects to- or above non-OI untreated control levels. Acute inhibition of sclerostin induced an upregulation of inhibitory regulators (*SOST, DKK1*) similar to prior reports in animal models treated with SclAb. The sample's untreated gene expression appeared to influence the magnitude of response to SclAb treatment, specifically for osteoblast and osteoblast progenitor genes *COL1A1*, *RUNX2*, *SP7* and *BGLAP*. We observed that OI bone samples with low untreated expression of a gene targeted by SclAb generally demonstrated a greater magnitude of response (upregulation) with treatment. Conversely, samples with higher untreated gene expression elicited moderate to minimal upregulation with sclerostin inhibition. Gene expression at the time of treatment may provide new insights in predicting treatment response and guide clinical decision making in OI. Due to the rarity of the tissue, we were unable to attribute whether the variability in baseline conditions is attributed to anatomic site, bone type, OI subject type, sex, or age.

Our findings in human pediatric OI tissue share similarities with studies monitoring gene expression treatment response to SclAb in animal models of bone loss. Nioi et al. evaluated expression

changes in 84 confirmed canonical *Wnt* target genes in OVX rats treated with SclAb and reported significant upregulation in a focused set of *Wnt* targets: *Wisp1*, *Twist1*, *Bglap*, *Gja1* and *Mmp2*. The authors reported the most consistent SclAb treatment response was observed in the *Wisp*/*Twist* cluster. [39] In our patient tissue, SclAb induced an upregulation of *WISP1* and *TWIST1*.with the greatest upregulation in samples with low untreated expression in the *WISP*/*TWIST* cluster. *WISP1* and *TWIST1* hold important roles in modulating osteogenesis and cell function. *WISP1* has been described to act as a negative regulator of osteoclastogenesis and its upregulation following SclAb treatment may point to its proposed anti-resorptive effects. [49] While *TWIST1*'s function is not as well defined, the gene is thought to serve as a negative regulator of *RUNX2* and an upregulation in *TWIST1* is suggestive of *RUNX2* inhibition (a marker of bone formation).[50] Supporting *TWIST1*'s proposed role, OI1 demonstrated a large upregulation in *TWIST1* and a concurrent downregulation of *RUNX2* with treatment (**Figure 4**). It has additionally been proposed that *TWIST1* may be responsible for the inhibition of osteoblast apoptosis by suppressing *TNF-α* but *TNF-α* was not quantified in the present study. [51]

SclAb stimulates a rapid increase in bone formation in preclinical models [33, 34, 52, 53] and increases markers of bone formation, increases BMD, [54] decreases vertebral fracture risk [30] and increases trabecular and cortical bone mass [56] in patients with low bone mass. Nioi et al. observed that *Bglap* and *Col1a1* were significantly upregulated in osteoblast lineage cells following one dose of SclAb in an OVX rat model indicating a bone forming response can be both acute and robust. [39] Our findings are supportive of Nioi et al. and others where we observed that SclAb treatment elicited an early bone-forming response through upregulation of *COL1A1* and *BGLAP* in nearly all treated OI samples. [39, 43,

57] This upregulation following short-term treatment reflects initial stages of bone anabolism consistent with an eventual increase in osteoblast differentiation. Taken together with *WISP1* upregulation, results suggest an increase in bone forming activity and evidence of a concurrent decrease in resorptive activity. We observed an upregulation in *RANKL* (albeit slight) and down regulation in *OPG* which align with Stolina et al. where no changes in *Rankl* or *Opg* were observed following SclAb treatment in aged OVX rats. [40] However, Stolina et al. evaluated *Rankl* and *Opg* expression following long-term treatment, not short-term as in the present study, where treatment-induced bone forming gains may have begun to attenuate as previously described. [52, 58, 59] Alternatively, it is possible that the inconsistent results in our *in vitro* model compared to animal models treated with SclAb may be due in part to the unloaded condition experienced during culture which may have led to *RANKL* upregulation.[60] We acknowledge, however, that the OI condition may also mirror disuse. Future studies could evaluate the *in vitro* treatment response in human OI tissue under *in vitro* loading conditions in order to induce mechanotransduction in the bone to determine the impact on *RANKL* and *OPG*. [61]

Following long-term SclAb treatment, bone formation begins to attenuate or decrease, suggesting a period where the bone begins to self-regulate the anabolic action. [38, 52, 57-59] It has been proposed that the dampening effects following long-term SclAb treatment may be due to a large and acute upregulation in inhibitory regulators of bone formation (*SOST, DKK1*).[37] We observed a similar upregulation of *SOST* and *DKK1* with SclAb treatment. This compensatory response has been documented in the acute phase of treatment with significant upregulation observed following a single dose of SclAb. [37] Because SclAb acts to prevent the interaction of sclerostin with LRP5/6, not by blocking the production of sclerostin, it has been suggested that a signaling event may occur to increase

secretion of sclerostin following the initial blocking of LRP5 binding. [62] This event may lead to an increase in inhibitory regulators leading to the observed compensatory upregulation in *SOST* and *DKK1* we observed in order to regulate the concurrent early bone-formation gains.

While SclAb elicited increases in osteoblast and osteoblast progenitor markers and increases in inhibitory regulators in our OI tissue, the magnitude of this response varied across samples. Variability in treatment response has been observed clinically with no clear causation documented and no metric to predict which patients will positively respond to a therapy and which patient will require a completely different treatment approach to mitigate the effects of the disease. OI type, phenotypic severity and age provide valuable guides when determining a treatment plan but identification of factors that contribute to differential treatment response would be advantageous. For example, following two years of Pamidronate treatment in children with Type III and Type IV OI, Zacharin et al. reported no statistical correlation in age, phenotypic severity, or predicted collagen mutation on treatment response.[24] While nearly all patients in the study demonstrated improvements in BMD, magnitude of BMD gains differed between and within patients of the same OI type. We demonstrated that SclAb response statistically differed between OI Type (III, IV, III/IV) in key inhibitory genes (*SOST*, *DKK1*, *TWIST1*) and for osteoblast markers (*RUNX2*). Specifically, patients with OI Type III, considered the most severe form of children who survive through the neonatal period, demonstrated the greatest upregulation in these markers with treatment. It is understood that severity of the disease can vary within OI type. When treatment response was evaluated between individual patients, the magnitude of response differed *within* patients of the same OI classification suggesting factors beyond phenotype may be responsible for differential treatment response.

When normalized to the average non-OI untreated control, we observed a differential expression in all genes evaluated among the seven OI samples. This variability in the untreated condition was present irrespective of OI type or bone origin. Interestingly, when OI tissue was treated with SclAb, untreated expression of bone formation markers appeared to impact the magnitude of response during our short-term treatment *in vitro*. Bone with the lowest relative untreated expression of osteoblast and osteoblast precursor markers *SP7*, *RUNX2*, *COL1A1* and *BGLAP* were particularly impacted demonstrating the greatest upregulation following treatment. In contrast, samples with a high relative untreated expression of these markers, indicative of a bone forming response, were only moderately upregulated when treated with SclAb. From our results, we postulate that there is an upper limit for eliciting an early/rapid bone response with SclAb which is perhaps attributable to 1) the amount of available mesenchymal stem cells (MSCs) and quiescent bone lining cells [57, 63, 64] and 2) the available bone surface area for which osteoblasts can differentiate. We can reason that bone sites with high expression levels of osteoblast markers and osteoblast progenitors have "little room" for further formation where further minimal upregulation was observed. Second, there is a finite bone surface area in which SclAb can induce bone formation (without the use of co-treatment of bisphosphonate, for example [65, 66] and perhaps a maximization of bone forming surfaces in the sample had already occurred, further limiting bone response. Future work should evaluate these potential factors, including evaluating bone turnover markers (*P1NP*, *TNSAP*) and their role in determining the magnitude of treatment response. To decrease site-specific variability in samples, future studies should attempt to standardize bone harvest site, such as obtaining specimens from iliac crest biopsies. While these locations may have a distinctly different mechanical loading environment than sites sampled here, they

represent a sampling area that has previously been used to characterize OI phenotype through histomorphometric assessment {Rauch, 2000 #68}.

The *in vitro* environment provides a safe and reductionist method to evaluate human tissue response to SclAb but the environment is limited in both biokinetic and metabolic factors inherent to the *in vivo* environment. We extended treatment to human bone from three OI patients *in vivo* using a xenograft model to evaluate the bone forming response to SclAb in an environment that more closely recapitulates the patient environment. [42] We implanted both cortical-derived (OI3 and OI6) and trabecular-derived tissue (OI4) and observed a greater magnitude of response to SclAb in trabecular-derived implants following two weeks of treatment in both μCT and histomorphometry outcomes. For OI4, trabecular-derived implants, this response appeared to attenuate following four weeks of treatment where μCT changes measured from pre- to post- treatment decreased in magnitude compared to the two week treated implants from the same patient. Because of the limited bone tissue we received from patients OI3 and OI6, we did not allocate tissue to the four week treated time point (instead, using the tissue for *in vitro* analysis), so we did not evaluate treatment response in the cortical implants at four weeks. Our first description using this xenograft demonstrated that cortical-derived bone with minimal human marrow cells at the time of implantation requires longer implantation duration to elicit a bone-forming response and that trabecular derived- implanted patient tissue demonstrates a greater magnitude of response.[42] When the parallel cortical-derived bone tissue from OI3 and OI6 were treated acutely *in vitro*, we did observe an upregulation in osteoblast markers (particularly *SP7*) and an upregulation (compensatory response) in inhibitory regulators *SOST* and *DKK1* indicating a treatment response. Future analysis using the proposed xenograft model should evaluate gene expression response analogous

to the panel reported in the present study to determine the effects of SclAb in the host-derived microenvironment in comparison to the *in vitro* response.

Limitations

There are several limitations to this study. We evaluated expression levels in OI patient bone tissue removed during corrective orthopaedic procedure using qPCR to quantify a panel of key genes involved in bone metabolism. We are therefore evaluating a specific point in time for these patients; it is both feasible and likely that expression levels will continue to change with growth and in consequence to environmental factors in this pediatric population. In addition, and because of the rarity of the disease and tissue, we took bone from patients who were pre, peri, and post-pubescent. We therefore likely captured bone when it was undergoing a cellular range of modeling to remodeling, adding to the complexity of the study. However, these same challenges are representative of the challenges faced by treating physicians of patients with OI across age span. We were unable to standardize bone harvest site in the present study; instead, this rare pediatric bone tissue was taken as surgical waste from patients undergoing corrective orthopaedic procedure. Given this, we likely selected for more severe patients, as well as more severe sites, and were unable to compare to patients or anatomic sites not needing immediate surgical or medical attention. As indication for surgery varied across patients, so did the site of bone harvest. We did consider bone morphological type (trabecular- or cortical-derived) in our evaluation of treatment response. As such, it is feasible that expression levels varied by bone site within the same patient and site variation likely played a role in the untreated expression levels observed between OI patients and the magnitude of treatment response. Even so we believe this variation was not

a critical factor when evaluating treatment response *within* the patient where treatment response was normalized to that patient's untreated gene expression in samples harvested from the same site. Furthermore, we recruited all OI patients which qualified for the study and did not differentiate findings based on sex. Differences in expression levels could exist between male and female patients. Regarding response to treatment, unpublished work in our lab has determined that magnitude of response to SclAb does not differ between sex in the Brtl/- murine model. The amount of nucleic acid concentration, which was dependent on the amount of bone tissue harvested, limited the number of genes we were able to evaluate using TaqMan qPCR in some patients. This also inhibited the number of conditions we were able to evaluate; as such future studies should include a baseline or "time 0" condition where bone removed from the patient is immediately processed for qPCR. This should also be performed because the act of culturing the bone itself may have altered gene expression; culture lacks all the growth factors inherent to *in vivo* and therefore may have influenced untreated expression. While our focus was on an abbreviated panel of genes (a key panel we identified from prior pre-clinical work using SclAb), future studies should build on this work through RNA-sequencing (RNA-seq) of the treated rare OI tissue. RNA-seq provides more data overall and makes it possible to detect previously unknown transcripts, isoforms, junctions and evaluate genes in pathways where the user has little baseline knowledge on location that may be implicated by treatment. [67, 68]

Conclusions

Using solid tissue isolates from human OI bone patients *in vitro*, SclAb activates downstream *Wnt* targets of *WISP1* and *TWIST1* and induces a compensatory response in *SOST* and *DKK1* expression,

consistent with pre-clinical studies of ovariectomized rats and *SOST* and *DKK1* in female Balb/c mice. In all samples, a bone-forming response to treatment was observed but the magnitude of this response was variable. While OI type and bone origin (cortical, trabecular) were influential in response, the level of untreated gene expression appeared to greatly influence the magnitude of response to SclAb in native human OI bone tissue. Clinical heterogeneity is a hallmark of OI; understanding a patient's genetic, cellular and morphological bone phenotype may play an important role in predicting treatment response and could help guide clinical decision making.

Acknowledgements

We would like to gratefully acknowledge Dr. Christophe Merceron, Dr. Andrea Alford and Anita Reddy for the scientific guidance throughout the course of the study. We would like to thank Jaimee Gauthier, Richana Gaskin, and Aries Haflinger for their generous support during sample procurement. This material is based upon work supported by the National Science Foundation Graduate Research Fellowship Program under Grant No. 1256260 DGE (RKS). We would like to gratefully thank our funding sources: NIH AR062552, NIH AR069620, AR070903, MICHR NIH/NCATS UL1TR000433 and NSF-GRFP1256260 DGE. Amgen, Inc (Thousand Oaks, CA, USA) and UCB (Brussels, Belgium) graciously provided the SclAb.

Study Design: RS, MC, KMK. Data Collection: RS, SS, LB, EW, MC, KMK. Data Analysis: RS, LB, SS. Drafting Manuscript: RS, LB, SS, KMK. Approving final version of manuscript: RS, SS, LB, EW, MC, KMK. KMK takes responsibility for the integrity of the data.

References

1. Van Dijk, F.S. and D.O. Sillence, *Osteogenesis imperfecta: clinical diagnosis, nomenclature and severity assessment.* Am J Med Genet A, 2014. **164A**(6): p. 1470-81.
2. Kang, H., A.C.S. Aryal, and J.C. Marini, *Osteogenesis imperfecta: new genes reveal novel mechanisms in bone dysplasia.* Transl Res, 2017. **181**: p. 27-48.
3. Marini, J.C., et al., *Osteogenesis imperfecta.* Nat Rev Dis Primers, 2017. **3**: p. 17052.
4. Sillence, D.O. and D.L. Rimoin, *Classification of osteogenesis imperfect.* Lancet, 1978. **1**(8072): p. 1041-2.
5. Kaneto, C.M., et al., *Gene expression profiling of bone marrow mesenchymal stem cells from Osteogenesis Imperfecta patients during osteoblast differentiation.* Eur J Med Genet, 2017. **60**(6): p. 326-334.
6. Marini, J.C., et al., *Consortium for osteogenesis imperfecta mutations in the helical domain of type I collagen: regions rich in lethal mutations align with collagen binding sites for integrins and proteoglycans.* Hum Mutat, 2007. **28**(3): p. 209-21.
7. Brodsky, B., *Structural consequences of glycine missense mutations in osteogenesis imperfecta*, in *Osteogenesis Imperfecta: A Translational Approach to Brittle Bone Disease*, S. JR., Editor. 2013, Elsevier. p. 115-124.
8. Forlino, A., et al., *New perspectives on osteogenesis imperfecta.* Nat Rev Endocrinol, 2011. **7**(9): p. 540-57.
9. Cheung, M.S. and F.H. Glorieux, *Osteogenesis Imperfecta: update on presentation and management.* Rev Endocr Metab Disord, 2008. **9**(2): p. 153-60.
10. Forlino, A. and J.C. Marini, *Osteogenesis imperfecta.* Lancet, 2016. **387**(10028): p. 1657-71.
11. Lindert, U., et al., *MBTPS2 mutations cause defective regulated intramembrane proteolysis in X-linked osteogenesis imperfecta.* Nat Commun, 2016. **7**: p. 11920.
12. Symoens, S., et al., *Deficiency for the ER-stress transducer OASIS causes severe recessive osteogenesis imperfecta in humans.* Orphanet J Rare Dis, 2013. **8**: p. 154.
13. Volodarsky, M., et al., *A deletion mutation in TMEM38B associated with autosomal recessive osteogenesis imperfecta.* Hum Mutat, 2013. **34**(4): p. 582-6.
14. Alanay, Y., et al., *Mutations in the gene encoding the RER protein FKBP65 cause autosomal-recessive osteogenesis imperfecta.* Am J Hum Genet, 2010. **86**(4): p. 551-9.
15. Christiansen, H.E., et al., *Homozygosity for a missense mutation in SERPINH1, which encodes the collagen chaperone protein HSP47, results in severe recessive osteogenesis imperfecta.* Am J Hum Genet, 2010. **86**(3): p. 389-98.
16. van Dijk, F.S., et al., *PPIB mutations cause severe osteogenesis imperfecta.* Am J Hum Genet, 2009. **85**(4): p. 521-7.
17. Morello, R., et al., *CRTAP is required for prolyl 3- hydroxylation and mutations cause recessive osteogenesis imperfecta.* Cell, 2006. **127**(2): p. 291-304.
18. Martinez-Glez, V., et al., *Identification of a mutation causing deficient BMP1/mTLD proteolytic activity in autosomal recessive osteogenesis imperfecta.* Hum Mutat, 2012. **33**(2): p. 343-50.
19. Mendoza-Londono, R., et al., *Recessive osteogenesis imperfecta caused by missense mutations in SPARC.* Am J Hum Genet, 2015. **96**(6): p. 979-85.

20. Becker, J., et al., *Exome sequencing identifies truncating mutations in human SERPINF1 in autosomal-recessive osteogenesis imperfecta.* Am J Hum Genet, 2011. **88**(3): p. 362-71.
21. Morello, R., *Osteogenesis imperfecta and therapeutics.* Matrix Biol, 2018. **71-72**: p. 294-312.
22. Martin, E. and J.R. Shapiro, *Osteogenesis imperfecta:epidemiology and pathophysiology.* Curr Osteoporos Rep, 2007. **5**(3): p. 91-7.
23. Hald, J.D., et al., *Bisphosphonates for the prevention of fractures in osteogenesis imperfecta: meta-analysis of placebo-controlled trials.* J Bone Miner Res, 2015. **30**(5): p. 929-33.
24. Zacharin, M. and J. Bateman, *Pamidronate treatment of osteogenesis imperfecta--lack of correlation between clinical severity, age at onset of treatment, predicted collagen mutation and treatment response.* J Pediatr Endocrinol Metab, 2002. **15**(2): p. 163-74.
25. Drake, M.T., B.L. Clarke, and S. Khosla, *Bisphosphonates: mechanism of action and role in clinical practice.* Mayo Clin Proc, 2008. **83**(9): p. 1032-45.
26. Hoyer-Kuhn, H., et al., *Safety and efficacy of denosumab in children with osteogenesis imperfect--a first prospective trial.* J Musculoskelet Neuronal Interact, 2016. **16**(1): p. 24-32.
27. Ferrari-Lacraz, S. and S. Ferrari, *Do RANKL inhibitors (denosumab) affect inflammation and immunity?* Osteoporos Int, 2011. **22**(2): p. 435-46.
28. Trejo, P., F. Rauch, and L. Ward, *Hypercalcemia and hypercalciuria during denosumab treatment in children with osteogenesis imperfecta type VI.* J Musculoskelet Neuronal Interact, 2018. **18**(1): p. 76-80.
29. Recker, R.R., et al., *A randomized, double-blind phase 2 clinical trial of blosozumab, a sclerostin antibody, in postmenopausal women with low bone mineral density.* J Bone Miner Res, 2015. **30**(2): p. 216-24.
30. Cosman, F., et al., *Romosozumab Treatment in Postmenopausal Women with Osteoporosis.* N Engl J Med, 2016. **375**(16): p. 1532-1543.
31. Glorieux, F.H., et al., *BPS804 Anti-Sclerostin Antibody in Adults With Moderate Osteogenesis Imperfecta: Results of a Randomized Phase 2a Trial.* J Bone Miner Res, 2017. **32**(7): p. 1496-1504.
32. Sinder, B.P., et al., *Effect of anti-sclerostin therapy and osteogenesis imperfecta on tissue-level properties in growing and adult mice while controlling for tissue age.* Bone, 2016. **84**: p. 222-229.
33. Sinder, B.P., et al., *Rapidly growing Brtl/+ mouse model of osteogenesis imperfecta improves bone mass and strength with sclerostin antibody treatment.* Bone, 2015. **71**: p. 115-23.
34. Sinder, B.P., et al., *Sclerostin antibody improves skeletal parameters in a Brtl/+ mouse model of osteogenesis imperfecta.* J Bone Miner Res, 2013. **28**(1): p. 73-80.
35. Grafe, I., et al., *Sclerostin Antibody Treatment Improves the Bone Phenotype of Crtap(-/-) Mice, a Model of Recessive Osteogenesis Imperfecta.* J Bone Miner Res, 2016. **31**(5): p. 1030-40.
36. Roschger, A., et al., *Effect of sclerostin antibody treatment in a mouse model of severe osteogenesis imperfecta.* Bone, 2014. **66**: p. 182-8.
37. Holdsworth, G., et al., *Dampening of the bone formation response following repeat dosing with sclerostin antibody in mice is associated with up-regulation of Wnt antagonists.* Bone, 2018. **107**: p. 93-103.
38. Taylor, S., et al., *Time-dependent cellular and transcriptional changes in the osteoblast lineage associated with sclerostin antibody treatment in ovariectomized rats.* Bone, 2016. **84**: p. 148-159.
39. Nioi, P., et al., *Transcriptional Profiling of Laser Capture Microdissected Subpopulations of the Osteoblast Lineage Provides Insight Into the Early Response to Sclerostin Antibody in Rats.* J Bone Miner Res, 2015. **30**(8): p. 1457-67.

40. Stolina, M., et al., *Temporal changes in systemic and local expression of bone turnover markers during six months of sclerostin antibody administration to ovariectomized rats.* Bone, 2014. **67**: p. 305-13.
41. Feldman, A.T. and D. Wolfe, *Tissue processing and hematoxylin and eosin staining.* Methods Mol Biol, 2014. **1180**: p. 31-43.
42. Surowiec, R.K., et al., *A xenograft model to evaluate the bone forming effects of sclerostin antibody in human bone derived from pediatric osteogenesis imperfecta patients.* Bone, 2020. **130**: p. 115118.
43. Ma, Y.L., et al., *Time course of disassociation of bone formation signals with bone mass and bone strength in sclerostin antibody treated ovariectomized rats.* Bone, 2017. **97**: p. 20-28.
44. Taihi, I., et al., *Validation of Housekeeping Genes to Study Human Gingival Stem Cells and Their In Vitro Osteogenic Differentiation Using Real-Time RT-qPCR.* Stem Cells Int, 2016. **2016**: p. 6261490.
45. Rauh, J., A. Jacobi, and M. Stiehler, *Identification of stable reference genes for gene expression analysis of three-dimensional cultivated human bone marrow-derived mesenchymal stromal cells for bone tissue engineering.* Tissue Eng Part C Methods, 2015. **21**(2): p. 192-206.
46. Livak, K.J. and T.D. Schmittgen, *Analysis of relative gene expression data using real-time quantitative PCR and the 2(-Delta Delta C(T)) Method.* Methods, 2001. **25**(4): p. 402-8.
47. Yuan, J.S., et al., *Statistical analysis of real-time PCR data.* BMC Bioinformatics, 2006. **7**: p. 85.
48. Scientific, T., *Gene expression assay performance guaranteed with the TaqMan assays qPCR guarantee program. .* Applied Biosystems White Paper, 2015. **docs.appliedbiosystems.com/pebiodocs/088754.pdf**.
49. Maeda, A., et al., *WNT1-induced Secreted Protein-1 (WISP1), a Novel Regulator of Bone Turnover and Wnt Signaling.* J Biol Chem, 2015. **290**(22): p. 14004-18.
50. Yousfi, M., F. Lasmoles, and P.J. Marie, *TWIST inactivation reduces CBFA1/RUNX2 expression and DNA binding to the osteocalcin promoter in osteoblasts.* Biochem Biophys Res Commun, 2002. **297**(3): p. 641-4.
51. Yousfi, M., et al., *Twist haploinsufficiency in Saethre-Chotzen syndrome induces calvarial osteoblast apoptosis due to increased TNFalpha expression and caspase-2 activation.* Hum Mol Genet, 2002. **11**(4): p. 359-69.
52. Boyce, R.W., Q.T. Niu, and M.S. Ominsky, *Kinetic reconstruction reveals time-dependent effects of romosozumab on bone formation and osteoblast function in vertebral cancellous and cortical bone in cynomolgus monkeys.* Bone, 2017. **101**: p. 77-87.
53. Sinder, B.P., et al., *Adult Brtl/+ mouse model of osteogenesis imperfecta demonstrates anabolic response to sclerostin antibody treatment with increased bone mass and strength.* Osteoporos Int, 2014. **25**(8): p. 2097-107.
54. McClung, M.R. and A. Grauer, *Romosozumab in postmenopausal women with osteopenia.* N Engl J Med, 2014. **370**(17): p. 1664-5.
55. McClung, M.R., et al., *Romosozumab in postmenopausal women with low bone mineral density.* N Engl J Med, 2014. **370**(5): p. 412-20.
56. Graeff, C., et al., *Administration of romosozumab improves vertebral trabecular and cortical bone as assessed with quantitative computed tomography and finite element analysis.* Bone, 2015. **81**: p. 364-9.
57. Ominsky, M.S., et al., *Differential temporal effects of sclerostin antibody and parathyroid hormone on cancellous and cortical bone and quantitative differences in effects on the osteoblast lineage in young intact rats.* Bone, 2015. **81**: p. 380-391.

58. Boyce, R.W., et al., *Decreased osteoprogenitor proliferation precedes attenuation of cancellous bone formation in ovariectomized rats treated with sclerostin antibody.* Bone Rep, 2018. **8**: p. 90-94.
59. Li, X., et al., *Progressive increases in bone mass and bone strength in an ovariectomized rat model of osteoporosis after 26 weeks of treatment with a sclerostin antibody.* Endocrinology, 2014. **155**(12): p. 4785-97.
60. Moriishi, T., et al., *Osteocyte network; a negative regulatory system for bone mass augmented by the induction of Rankl in osteoblasts and Sost in osteocytes at unloading.* PLoS One, 2012. **7**(6): p. e40143.
61. Michael Delaine-Smith, R., et al., *Preclinical models for in vitro mechanical loading of bone-derived cells.* Bonekey Rep, 2015. **4**: p. 728.
62. Ke, H.Z., et al., *Sclerostin and Dickkopf-1 as therapeutic targets in bone diseases.* Endocr Rev, 2012. **33**(5): p. 747-83.
63. Kim, S.W., et al., *Sclerostin Antibody Administration Converts Bone Lining Cells Into Active Osteoblasts.* J Bone Miner Res, 2017. **32**(5): p. 892-901.
64. Ominsky, M.S., et al., *Tissue-level mechanisms responsible for the increase in bone formation and bone volume by sclerostin antibody.* J Bone Miner Res, 2014. **29**(6): p. 1424-30.
65. Olvera, D., et al., *Low Dose of Bisphosphonate Enhances Sclerostin Antibody-Induced Trabecular Bone Mass Gains in Brtl/+ Osteogenesis Imperfecta Mouse Model.* J Bone Miner Res, 2018. **33**(7): p. 1272-1282.
66. Perosky, J.E., et al., *Single dose of bisphosphonate preserves gains in bone mass following cessation of sclerostin antibody in Brtl/+ osteogenesis imperfecta model.* Bone, 2016. **93**: p. 79-85.
67. Agarwal, A., et al., *Comparison and calibration of transcriptome data from RNA-Seq and tiling arrays.* BMC Genomics, 2010. **11**: p. 383.
68. Malone, J.H. and B. Oliver, *Microarrays, deep sequencing and the true measure of the transcriptome.* BMC Biol, 2011. **9**: p. 34.

Tables

Table 1. Patient demographics and bone sample type.

Patient	Bone Sample Type *	Surgical Indication	Drug TR History	Harvest Location	Age/Sex	Ambulatory Status/Clinical Features	OI Type**	Bone Sample Yield
OI Patients								
OI 1	**Trabecular**	Revision	Depo-testosterone	L Ulna/Radius	17/M	Wheelchair; small stature	**III**	13
OI 2	**Cortical**	Osteotomy	None	R Tibia/Fibia	21/M	Wheelchair; small stature	**III**	10
OI 3	**Cortical**	Bilateral Osteotomies	None	R & L Femur	16 mos/F	Walks w/o assistance; normal stature	**III/IV**	5
OI 4	**Trabecular**	Osteoplasty & Nail Placement	Ca Citrate-Vitamin D3	R Femur	23/F	Walks w/o assistance; normal stature	**III/IV**	7
OI 5	**Trabecular**	Fracture	None	R Femur	16/M	Walks w/ periodic wheelchair use; normal stature	**III/IV**	14
OI 6	**Cortical**	Fracture	None	R Femur	2/F	Walks w/o assistance; normal stature	**III/IV**	7
OI 7	**Trabecular**	Fracture	None	L Femur	6/F	Walks w/o assistance; abnormal gait; small stature	**IV**	8
Average Non-OI Patients (N=5)								
Non-OI 1-5	**Morselized**	ACL Reconstruction	N/A	Tibial Reaming	Mean: 12 yrs; Range: 10-15 yrs; F=2, M=3	Normal gait prior to injury	**Unaffected**	Total: 51

*Color-coded by bone sample type; colors correspond to bar colors in **Figure 3 and 4**. **Color coded by OI Sillence Type classification; colors correspond to bar colors in **Supplemental Figure 1 and 2.**

Table 2. Target genes.

Role	Target Gene	TaqMan Assay ID
Inhibitory Regulators / Downstream *Wnt*	*SOST, DKK1, TWIST1, WISP1*	Hs00228830_m1, Hs00183740_m1, Hs01675818_s1, Hs01675818_s1
Osteoblastogenesis	*SP7, RUNX2*	Hs01866874_s1, Hs01047973_m1
Osteoblast Markers	*BGLAP, COL1A1*	Hs01587814_g1, Hs00164004_m1
Osteoclast Differentiation	*OPG, RANKL*	Hs00900358_m1, Hs00243522_m1
Housekeeping	*HPRT1*	Hs02800695_m1

Figures

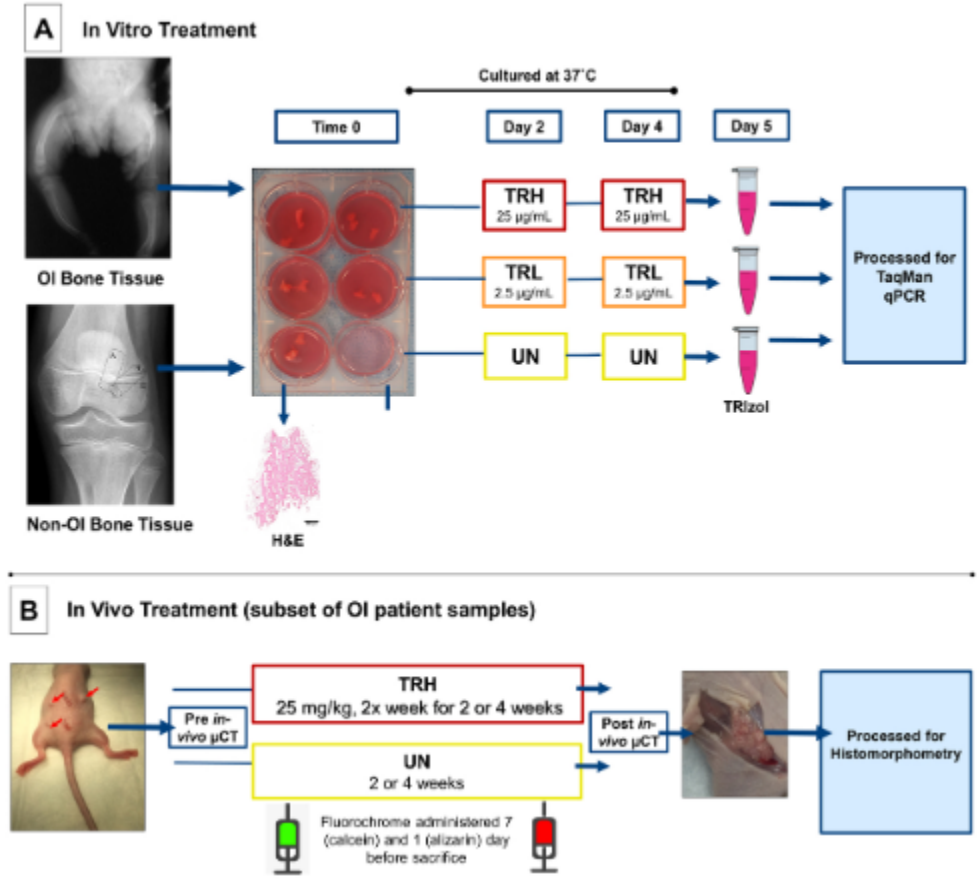

Figure 1. A. Cortical and trabecular bone samples (~2 mm^3 size per sample with each patient yielding up to 14 usable bone fragments) from osteogenesis imperfecta (OI) patients and morselized trabecular bone samples from non-OI control patients typically discarded as surgical waste during corrective orthopaedic procedures were collected to media and randomly assigned: untreated (UN), low-dose SclAb (TRL, 2.5 µg/mL), or high-dose SclAb (TRH, 25 µg/mL) group and maintained in culture (37ºC). Group assignment was as such that each group contained equal number of samples depending on patient yield with each 6 well plate generally containing between 2-3 ~2mm^3 bone fragments. Treatment

occurred on day 2 and 4 and samples were removed on day 5 for RNA extraction. One bone sample per patient was formalin-fixed upon harvest for baseline hematoxylin and eosin (H&E). B. A subset of OI bone tissue (14 samples from 3 OI patients) was immediately implanted subcutaneously on the dorsal surface (~2 mm^3 in size) of an athymic mouse representing our xenograft model. Implanted mice were randomly assigned to an UN or high dose (TRH, 25 mg/kg) group for 2 or 4 weeks where SclAb treatment was administered via subcutaneous injection 2 times a week. All mice received calcein and alizarin fluorochrome injections 7 and 1 day prior to sacrifice, respectively. Mice were imaged via μCT 24 hours after implantation and immediately following sacrifice. Following imaging, implanted OI bone tissue was removed from the host and plastic processed for dynamic histomorphometry analysis. Patient radiograph provided by MSC.

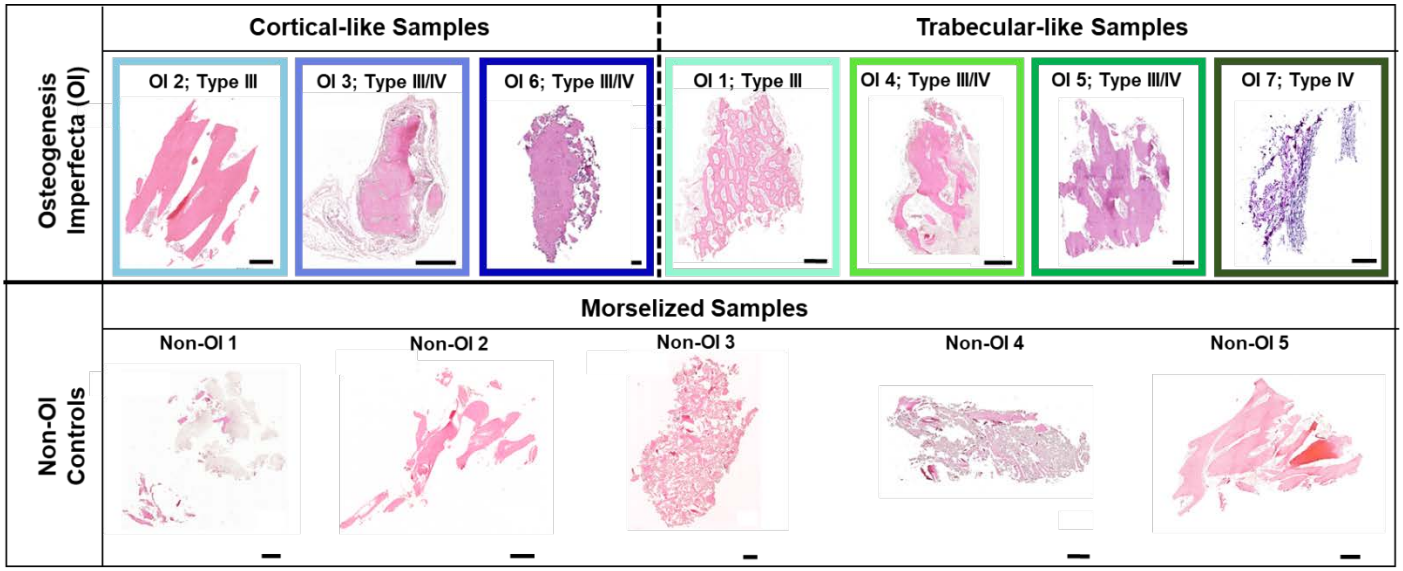

Figure 2. Patient donor bone tissue morphology for OI and non-OI patients were evaluated using hematoxylin and eosin (H&E). One bone sample per patient was not placed in culture but immediately formalin fixed, paraffin embedded and stained with H&E. For the OI patients, tissue ranged from cortical (OI2, OI3, OI6) and trabecular (OI1, OI4, OI5, OI7) bone tissue. In all cases, non-OI control bone tissue (bottom) was morselized trabecular bone due to the method it was removed during anterior cruciate ligament (ACL) reconstruction tibial tunnel placement (non-OI 1-5). Colored boxes surrounding OI patient samples correspond to subsequent figures depicting fold-change gene expression. Samples depicted are representative of bone samples used in the *in-vitro* assay. Images were acquired at 20x. Scale bar= 500 µm.

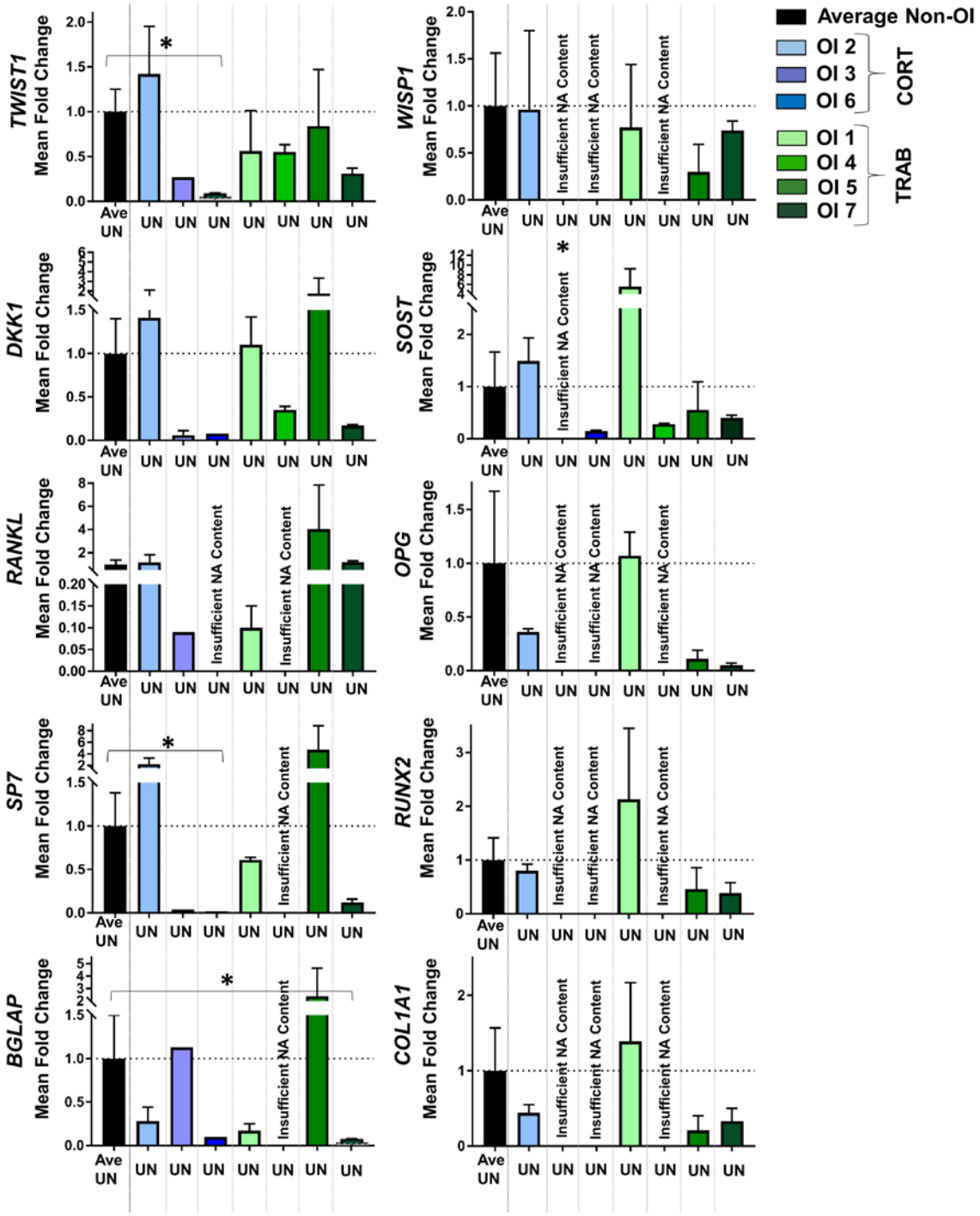

Figure 3. Quantification of fold-differences in the untreated expression of 10 genes of interest for each OI patient (n=7) normalized to the average untreated non-OI control patients (n=5) corrected by *HPRT1*. Height of bars represents fold-change derived from mean technical replicates and error bars represent standard error of the mean (SEM) derived from technical replicates of up to three pooled bone samples for the untreated condition for each OI patient. Untreated non-OI (black bar) is the average of these data from 5 patients. OI patients are organized by cortical-like bone samples (right, blue) and trabecular-like bone samples (left, green). [*] and brackets denote significant differences in OI expression compared to untreated controls at $p \leq 0.05$. Missing data due to insufficient nucleic acid content (NA) is indicated. UN= untreated; CORT=cortical-like samples; TRAB=trabecular-like samples.

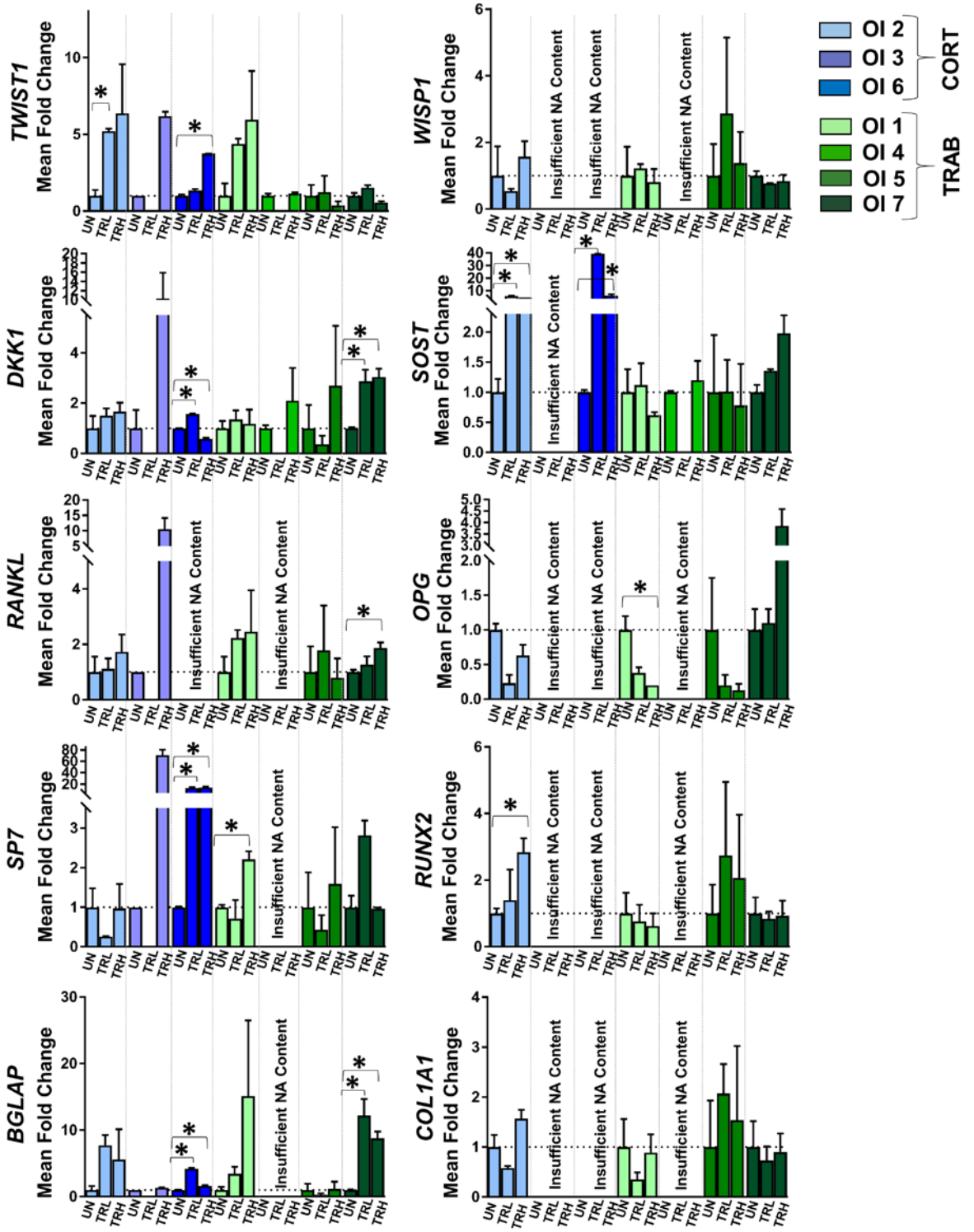

Figure 4. Quantification of fold-change expression of 10 genes of interest due to low (TRL) and high (TRH) dose SclAb treatment *in vitro*. Each OI patient's treated conditions were normalized to the individual patient's untreated condition, corrected by *HPRT1*. Height of bars represents relative fold-change derived from mean technical replicates and error bars represent standard error of the means (SEM) from technical replicates of up to three pooled bone samples for each condition (UN, TRL, TRH) for each OI patient (n=7). Data is organized by cortical-like patient samples (right, blue; OI2, OI3, OI6) and trabecular-like patient samples (left, green; OI1, OI4, OI5, OI7). [*] and brackets denote significance within each patient due to treatment at $p \leq 0.05$. Missing data due to insufficient nucleic acid (NA) content is indicated. UN=untreated; TRL=low dose treatment; TRH=high dose treatment; CORT=cortical-like samples; TRAB=trabecular-like samples.

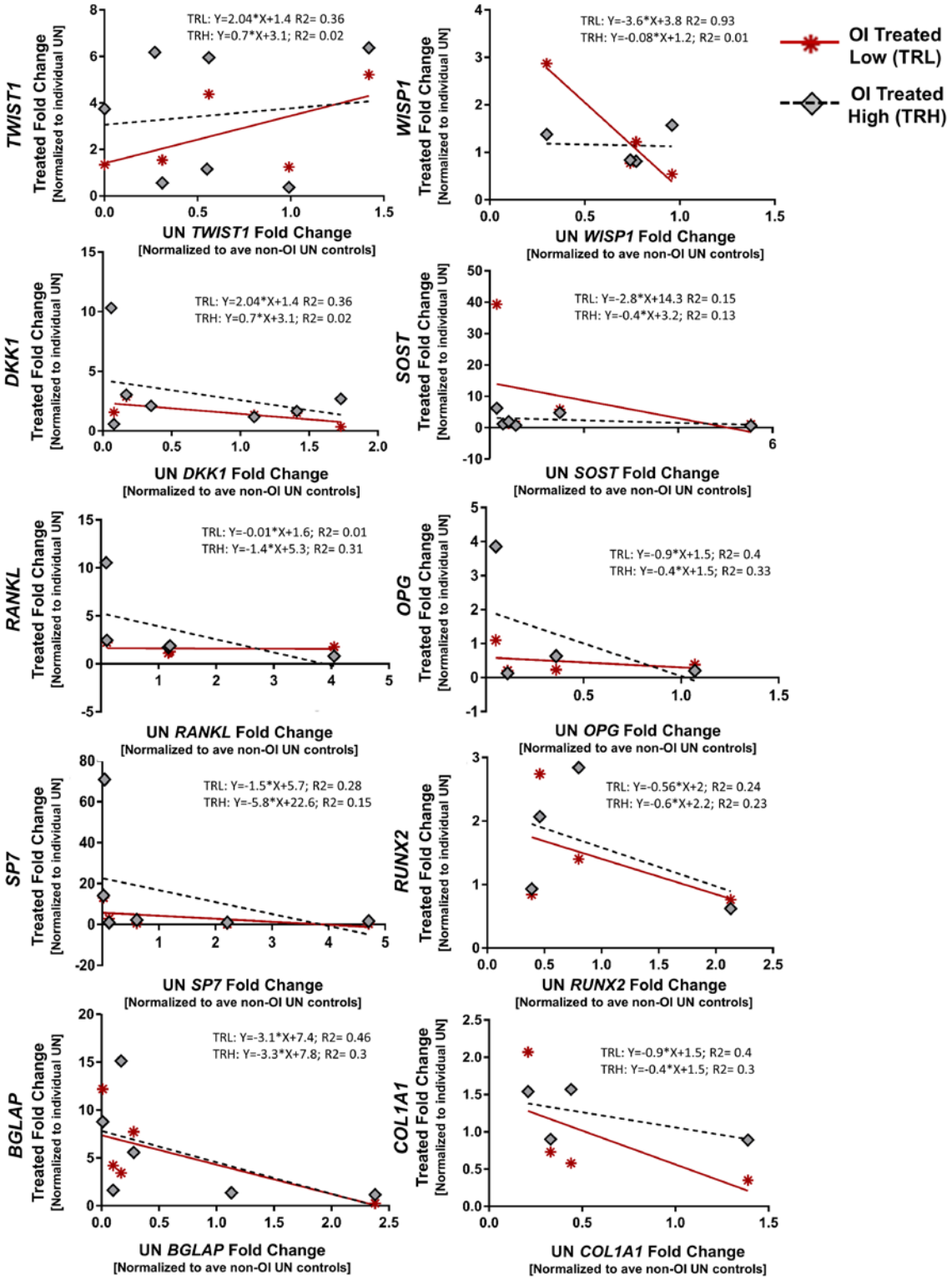

Figure 5. SclAb treated fold change for 10 genes of interest plotted against the individual patient's untreated fold change by dose (treated low dose, TRL; treated high dose, TRH). In particular, magnitude of treatment response of osteoblast markers and precursors *COL1A1*, *RUNX2*, *SP7* and *BGLAP* appeared to be impacted by the OI patient's relative untreated expression of the osteoblast related genes. SclAb treated OI patient bone that demonstrated a large magnitude of upregulation generally presented with low untreated expression. Conversely, patient bone that demonstrated little to no upregulation in osteoblast markers with SclAb treatment change due to treatment generally demonstrated high relative untreated expression of the gene of interest. Data represents treatment fold-change relative to the individual patient's untreated condition (Y-axis) plotted against the individual patient's untreated fold-change relative to the average non-OI control patients (X-axis). Specifically, each data point on the Y-axis represents individual OI-patient SclAb treated bone sample (TRL=red stars; TRH=grey diamonds) fold-change derived from technical replicates of three pooled condition bone samples normalized to the individual patient's untreated condition. X-axis is the individual patient's untreated fold-change condition normalized to the average non-OI untreated controls. TRL=treated low dose; TRH=treated high dose; UN=untreated; ave=average.

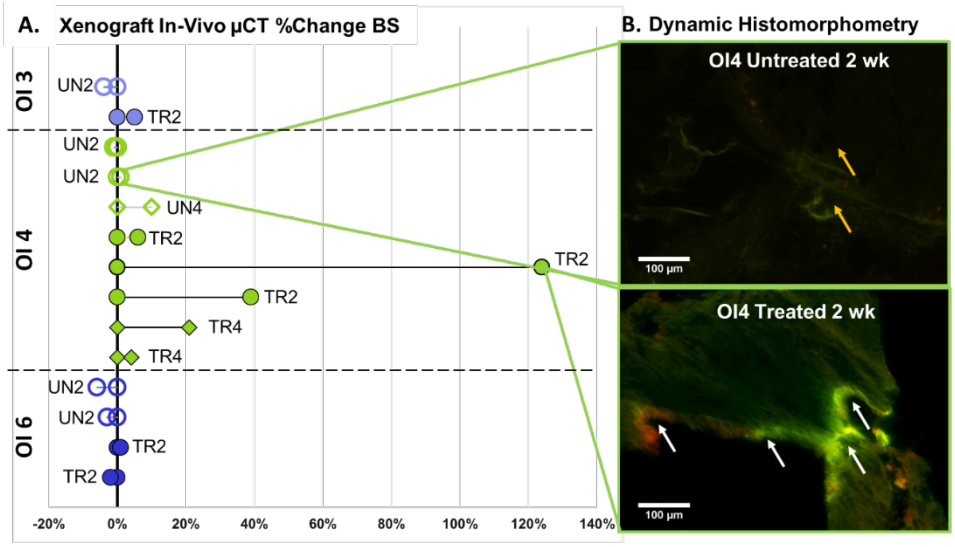

Figure 6. Due to the amount of patient bone procured, additional cortical-derived bone tissue from patient OI3 and OI6 and trabecular-derived bone tissue from patient OI4 were implanted subcutaneously into an athymic mouse representing our xenograft model system. A. OI implants treated with SclAb demonstrated increases in bone surface (BS) measured as a percent change from pre- to post- in vivo µCT following two weeks compared to untreated OI implants. B. Histomorphometry corroborated treatment-induced increases in BS at two weeks (bottom panel) demonstrating robust calcein (green) and alizarin (red) fluorochrome labeling (white arrows) compared to the untreated two week implants which had minimal non-specific calcein labeling only (yellow arrow). Fluorescent images acquired at 20x. Scale bar= 100 µm.

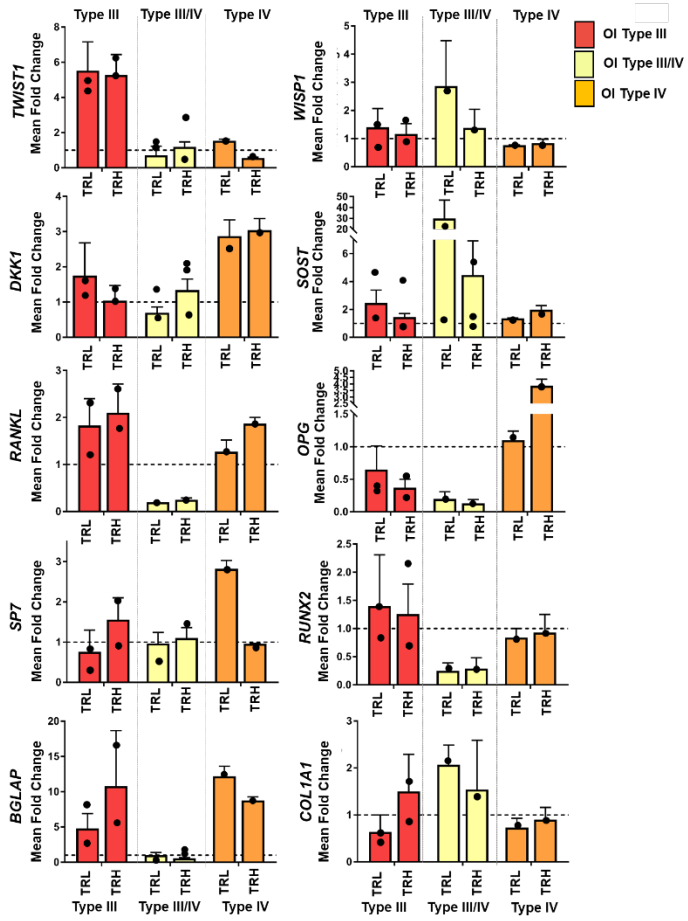

Supplemental Figure 1. Average fold-change expression of 10 genes of interest due to low (TRL) and high (TRH) dose SclAb treatment by patient's OI Sillence type clinical classification. Multiple bone tissue samples were harvested from patients clinically classified by physical examination and genetic testing as either Type III (n=2), Type III/IV (n=4) or Type IV (n=1). Average treated conditions for each OI type were normalized to average untreated condition for that OI type, corrected by HPRT1. For example, average TRL for all OI Type III patients were normalized to the average OI Type III untreated (UN) condition. Height of bars represents relative fold-change derived from combined mean technical replicates for all patients of that OI Type (each patient's technical replicates were averaged over

condition) and error bars represent standard error of the means (SEM) from averaged technical replicates which were derived from three pooled bone samples for each condition (UN, TRL, TRH) for each OI patient combined by OI type. Horizontal dotted line represents 1, or the normalized untreated condition and average treatment response (TRL and TRH) are plotted. Black circles represent individual OI patient fold change for each condition and correspond to results presented in **Figure 4**. Black circles indicate variability in treatment response to acute SclAb present within bone tissue obtained from patients of the same clinical OI classification. No significance was observed between UN, TRL and TRH conditions within OI type but difference in magnitude of treatment response by either increase or decrease in mean fold change gene expression can be appreciated between OI type.

A Two-Way ANOVA results of average condition by OI type normalized to average non-OI untreated controls

	TWIST1	*WISP1*	*SOST*	*DKK1*	*RANKL*	*OPG*	*SP7*	*RUNX2*	*BGLAP*	*COL1A1*
Treatment	0.08	0.86	**0.02**	0.81	0.70	0.57	0.92	0.96	0.53	0.79
Patient Type	**<0.0001**	0.34	**<0.0001**	**0.0002**	0.36	0.57	0.06	**0.01**	0.17	0.37
Interaction	0.07	0.71	**0.03**	0.65	0.56	0.88	0.77	0.95	0.22	0.93

B

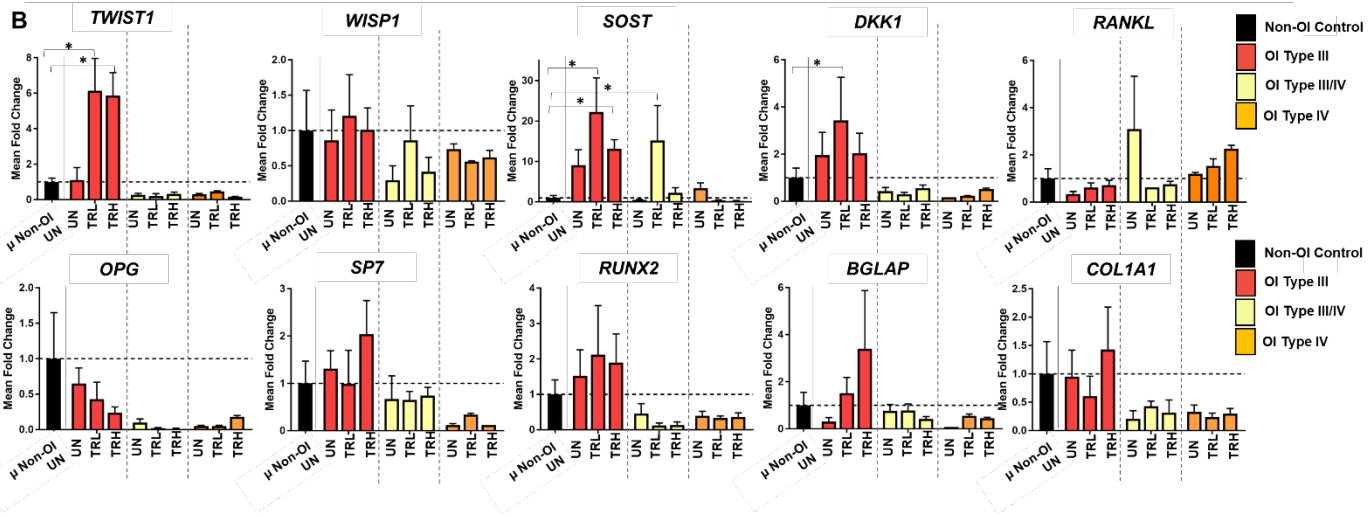

Supplemental Figure 2. A. Two-way non-repeated measures ANOVA results for each gene of interest comparing average treatment condition (UN, TRL, TRH) within OI type (Type III, Type III/IV, Type IV) normalized to average non-OI untreated control condition. Treatment and patient type served as factors and table values are bolded when significance was reached. B. Quantification of fold-change expression levels of 10 genes of interest for average OI Type III, average OI Type III/IV, and average OI Type IV patients in their untreated (UN) and SclAb treated low (TRL) and high (TRH) conditions. The average OI patient conditions were normalized to the average non-OI untreated condition, corrected by *HPRT1*, in order to create a common scale for the three OI patient populations. Height of bars represents relative fold-change derived from the average of each patients conditional (UN, TRL, TRH) mean technical replicates and error bars represent standard error of the means (SEM) from these

technical replicates of three pooled bone samples from each condition, for each patient. Data is organized by OI Type III patients (left, horizontal stripes) and OI Type IV patients (right, diagonal stripes). [*] and brackets denote significant difference from the non-OI untreated control using a Dunnett's post-hoc test at $p \leq 0.05$.

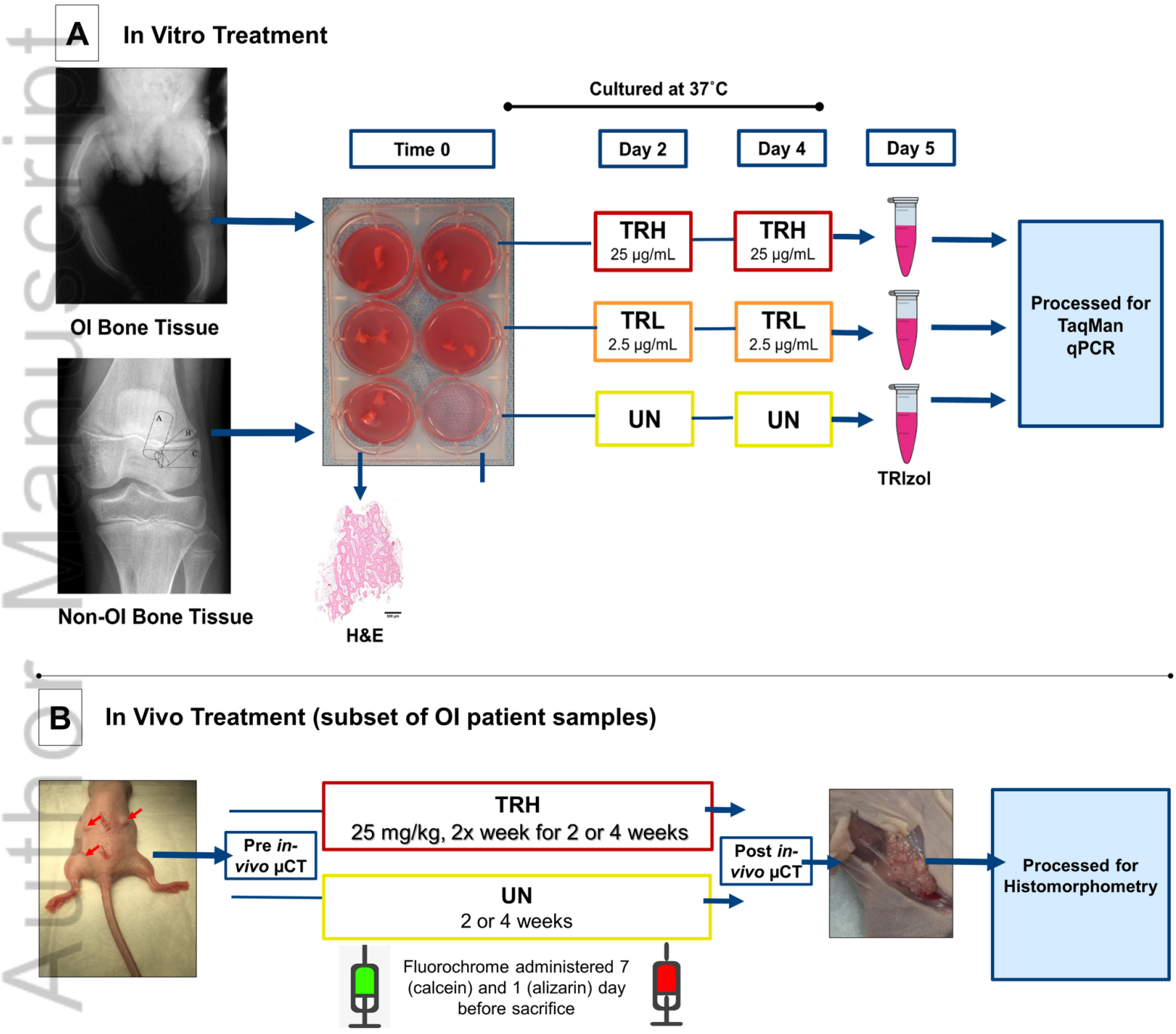

JBM4_10377_Figure 1_Study Schematic_Final.tif

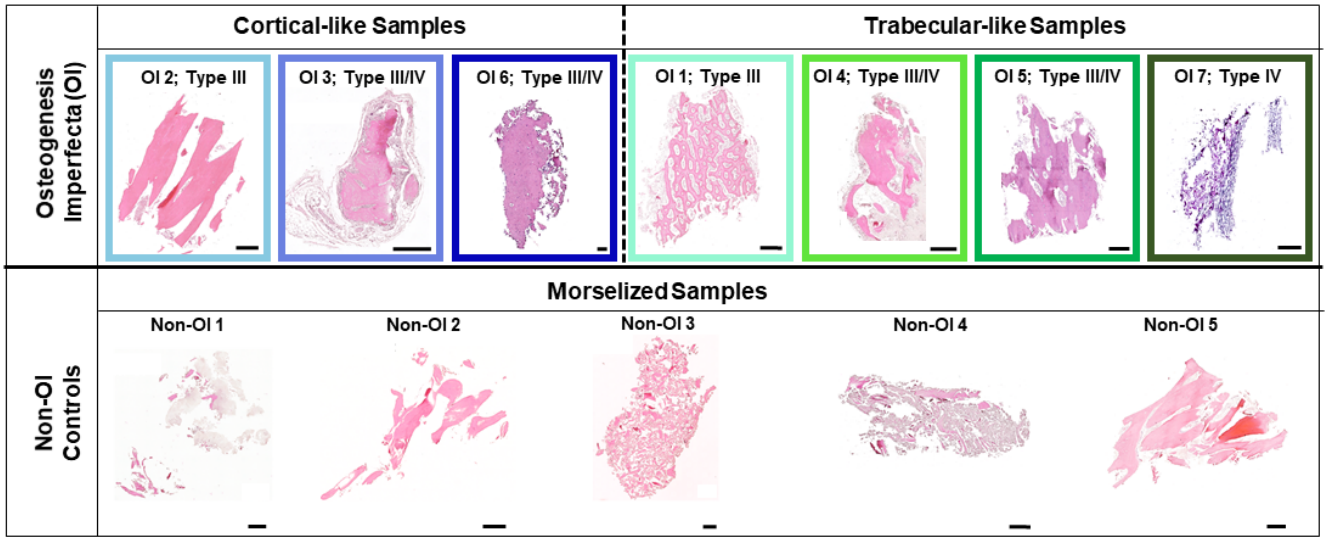

JBM4_10377_Figure 2_HE Panel_FINAL.tif

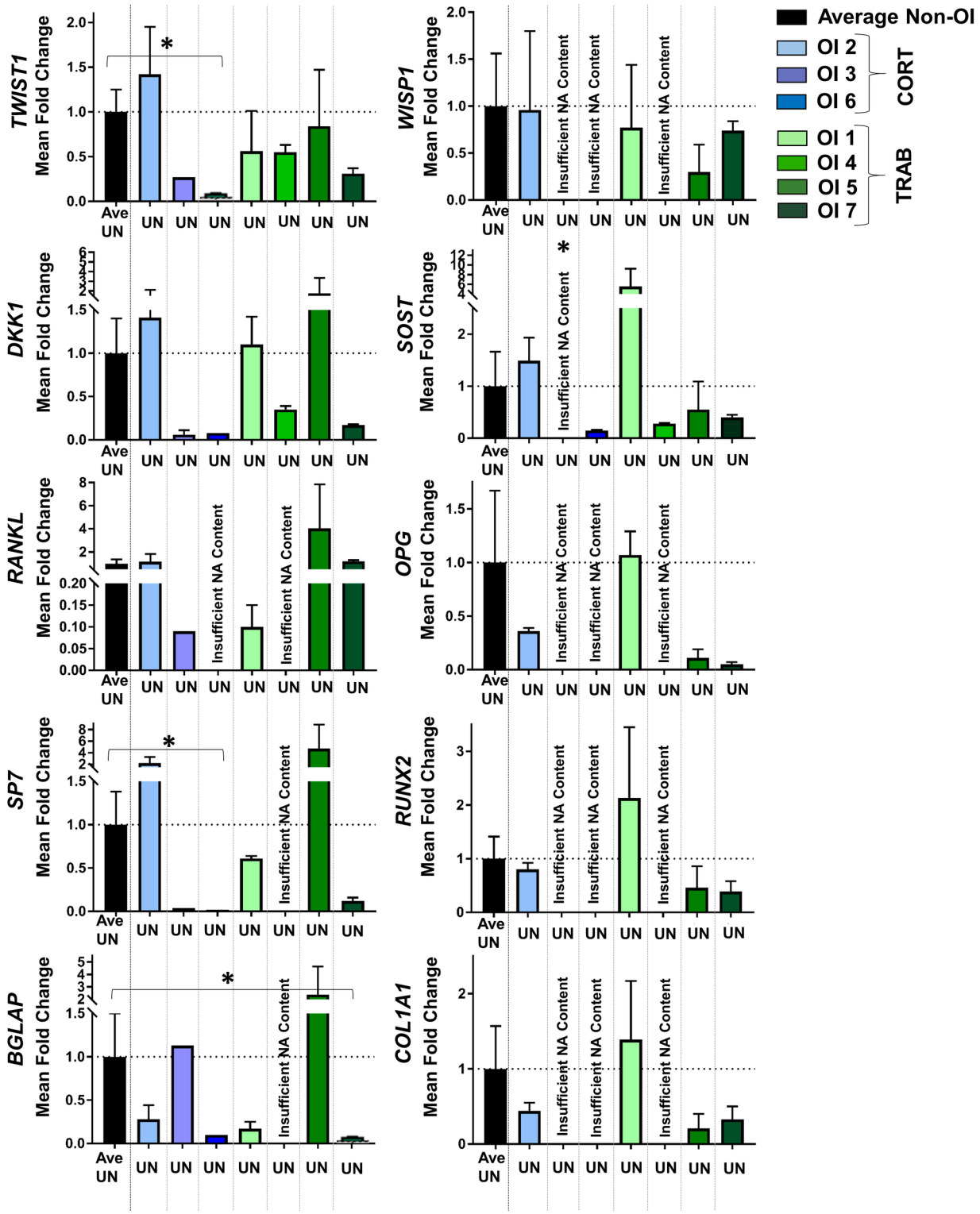

JBM4_10377_Figure 3_oi1-7 non oi 1-5 qPCR Figures_Color Coded Baseline.tif

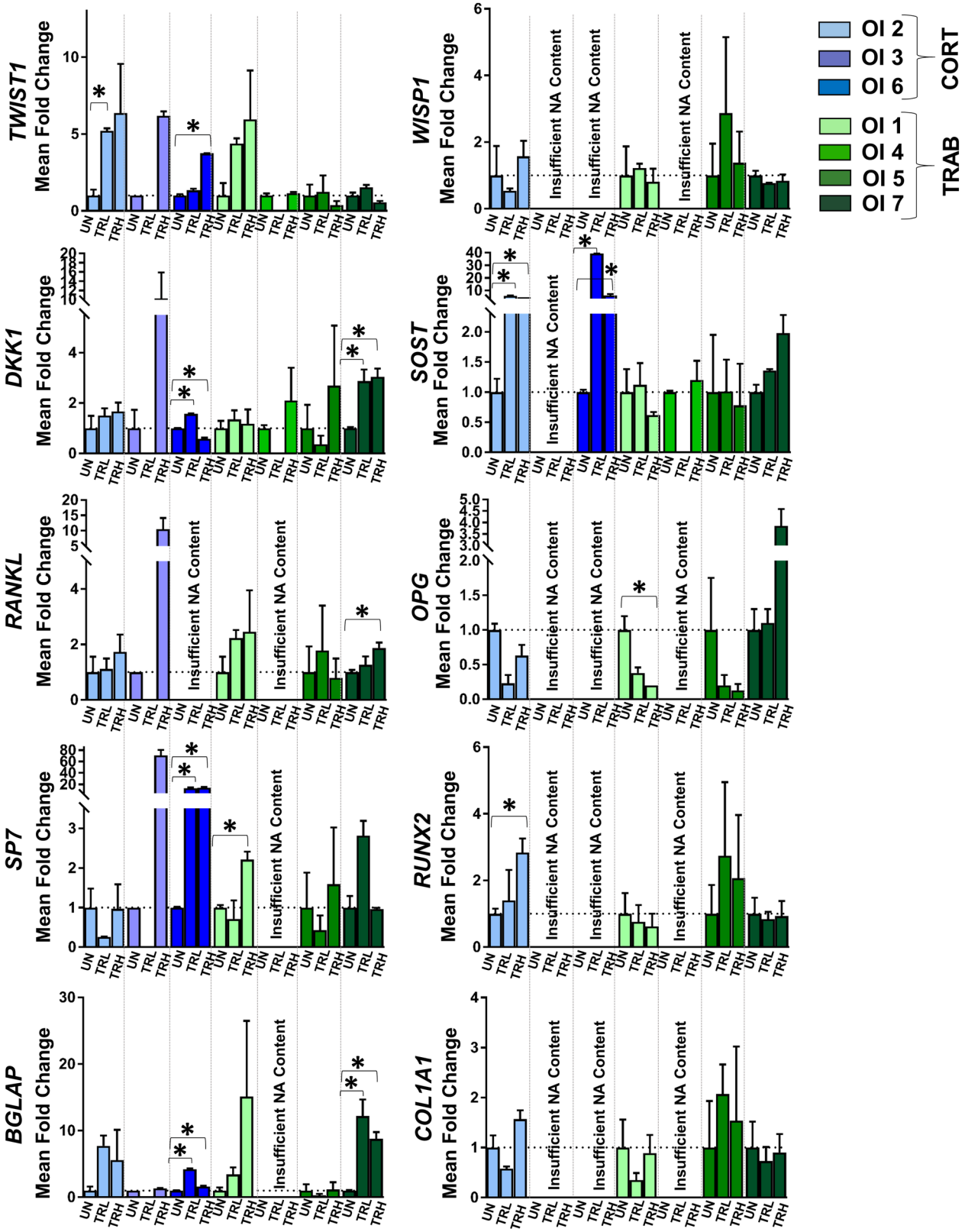

JBM4_10377_Figure 4_oi1-7 non oi 1-5 qPCR Figures_Color Coded Within TR.tif

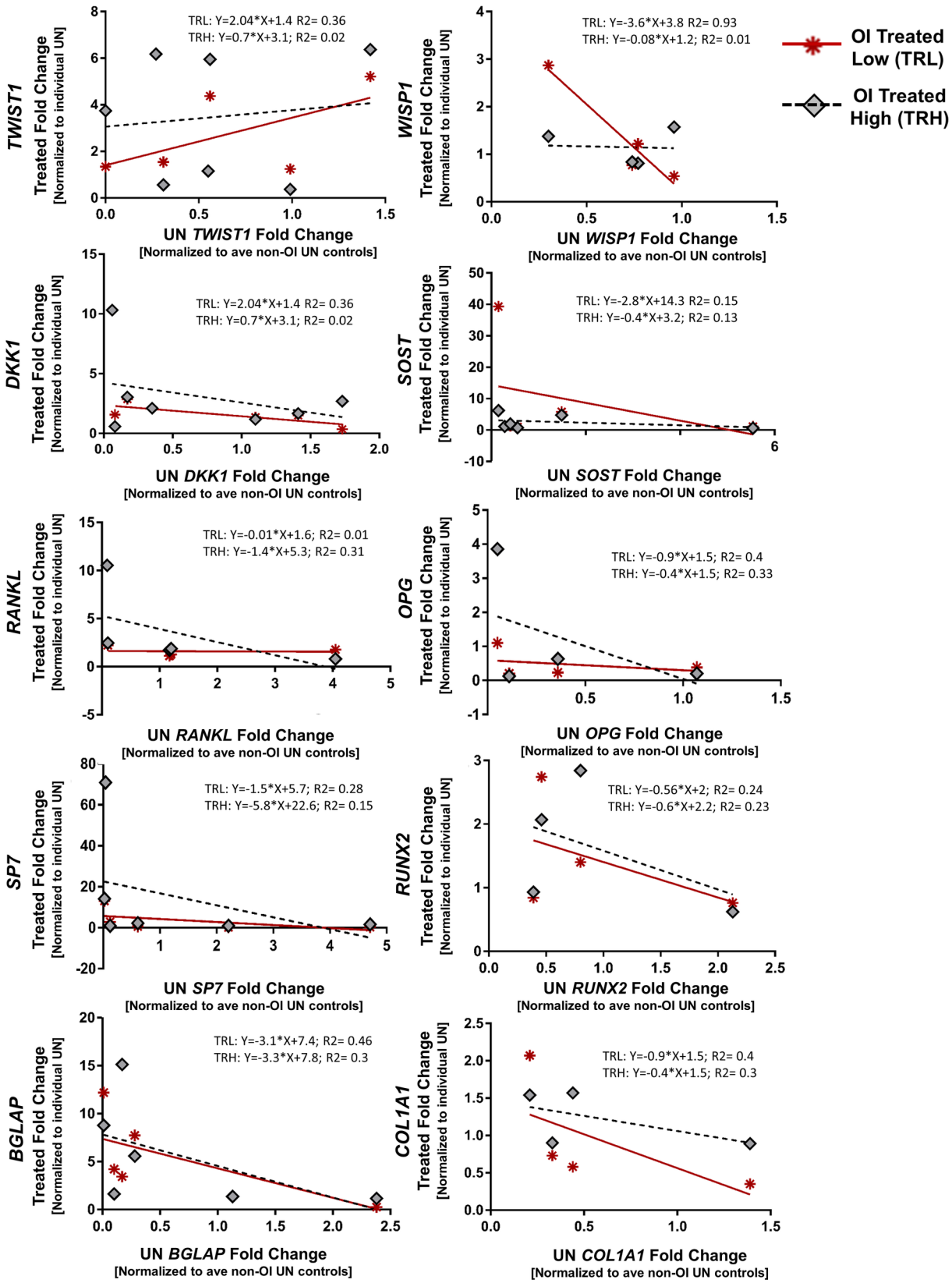

JBM4_10377_Figure 5_oi1-7 non oi 1-5 qPCR Figures_SCATTER PLOT.tif

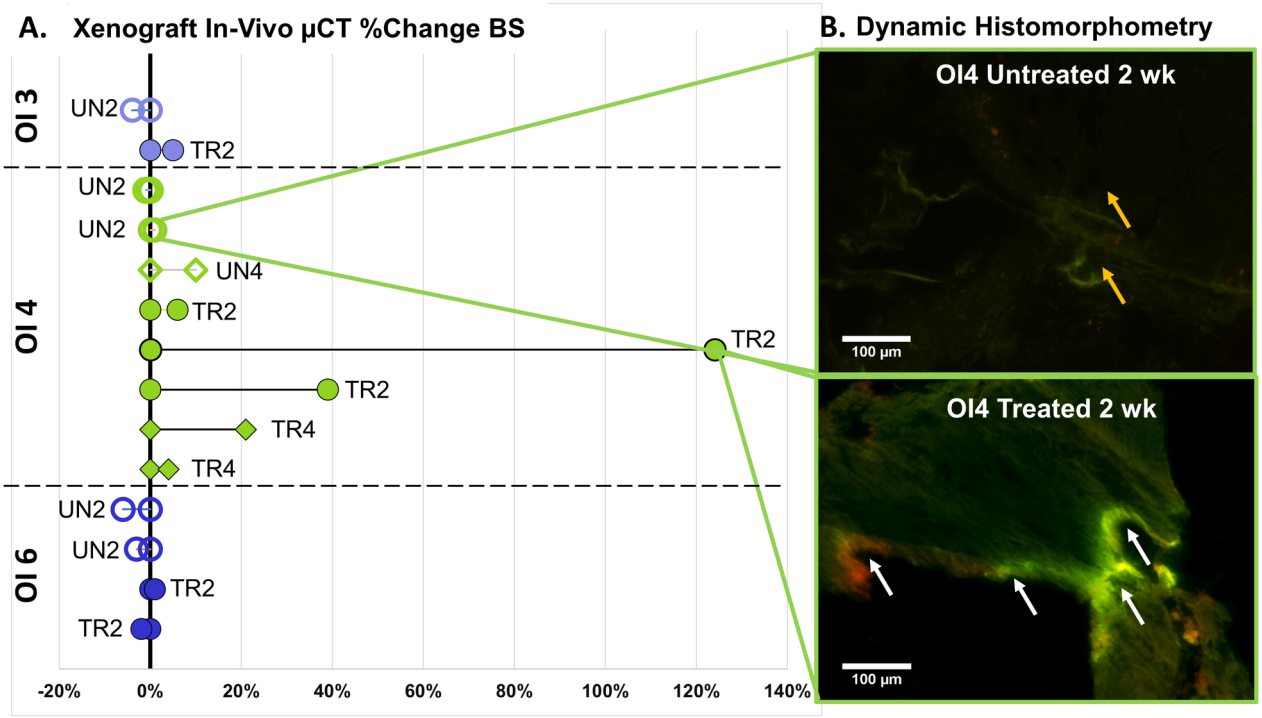

JBM4_10377_Figure 8_Xenograft uCT and Histomorphometry Data.tif